# Cooperative OFDM Channel Estimation in the Presence of Frequency Offsets

Zhongshan Zhang, *Member, IEEE*, Wei Zhang, *Student Member, IEEE*, and
Chintha Tellambura, *Senior Member, IEEE*

*Abstract*—Channel estimation in the presence of frequency offsets is developed for cooperative orthogonal frequency-division multiplexing (OFDM) systems. A two-time-slot cooperative channel estimation protocol is proposed. The source broadcasts the training sequence to the relays and the destination (first time slot), and the relays retransmit the training sequence (second time slot). Pilot designs for amplify-and-forward (AF) and decode-and-forward (DF) relays are derived. These designs eliminate interrelay interference (IRI), which occurs due to the simultaneous relay retransmissions, and minimize the mean square error (MSE). Consequently, the number of AF and DF relays is constrained to be less than $\lfloor N/(2L-1) \rfloor$ and $\lfloor N/L \rfloor$, respectively, where $N$ is the total number of subcarriers, $L$ is the channel order, and $\lfloor a \rfloor$ is the maximum integer part of $a$. The pairwise error probability (PEP) of orthogonal space–time coding in cooperative OFDM due to both frequency offset and channel-estimation errors is also evaluated. The optimal power allocation ratio between the source and the relays to minimize the PEP is derived for AF and DF relays. When $L < 16$, DF relays outperform AF relays in terms of PEP. With $L = 4$ and 16 active relays, the gap is 9 dB for a frequency offset error variance of $10^{-3}$, and this gap increases to about 11.3 dB when the variance increases to $10^{-2}$.

*Index Terms*—Amplify-and-forward (AF), channel estimation, cooperation, decode-and-forward (DF), frequency offset, orthogonal frequency-division multiplexing (OFDM).

## I. INTRODUCTION

COOPERATIVE relaying, where distributed multiple nodes form a virtual multiple-antenna array, has intensively been studied for wireless networks in recent years [1]–[3]. The use of relays may lead to expanded coverage, system-wide power savings, and better immunity against signal fading. It is expected that relay protocols will be used in beyond-third-generation (B3G) and fourth-generation (4G) systems [4]. Relays can be amplify-and-forward (AF) or decode-and-forward (DF). AF relays simply retransmit a linearly scaled (amplified) version of the received signal. Consequently, AF relays are not only transparent to any adaptive modulation employed by the source but also have low complexity and power consumption. DF relays (regenerative), on the other hand, demodulate and retransmit. Many relay studies focused on flat-fading channels, where single-carrier (SC) systems are of interest [5]–[8].

However, the use of relays in frequency-selective broadband channels is important as well. Of course, the popular solution against frequency-selective fading is orthogonal frequency-division multiplexing (OFDM). For instance, the IEEE 802.11n standard uses a physical layer based on multiple-input–multiple-output (MIMO) OFDM in the 2.4- and 5-GHz bands [9], [10]. Cooperative OFDM relay networks and cooperative orthogonal frequency-division multiple access (OFDMA) are, thus, increasingly important [11]–[14].

The performance of OFDM can significantly be impacted by frequency offsets. However, pervious studies [11], [12] do not consider the effect of frequency offset, which degrades the signal-to-interference-plus-noise ratio (SINR). Both the inter-symbol interference (ISI) and the intercarrier interference (ICI) mitigation in a cooperative space–frequency block-coded (SFBC) OFDM, by considering the frequency offset, are analyzed in [15]. The performance degradation of a cooperative OFDMA uplink due to the frequency offset is analyzed in [13], and the interference due to the effects of both timing and frequency offsets in OFDMA uplink is studied in [16].

Channel-estimation errors can also significantly impact the system performance. The AF channel statistics, which is not Gaussian, is analyzed in [17]. AF-SC channel estimation is discussed in [18]. Since relay networks are virtual MIMO systems [6], many existing MIMO channel-estimation algorithms, e.g., those proposed in [19]–[22], can also be adapted. Frequency offset estimation and channel estimation for cooperative MIMO sensor networks are discussed in [23], where the complexity is reduced by using a generalized successive interference cancellation (GSIC) algorithm. Per-subcarrier channel estimation for AF OFDM without frequency offset is studied in [24]. This method achieves the optimal Cramer–Rao lower bound (CRLB). Using Alamouti-coded pilot symbols, Shin *et al.* [25] provide synchronization and channel estimation for a cooperative OFDM system.

However, most of the existing algorithms are designed for SC relay networks (see [6] and [18]). For cooperative OFDM channel estimation, the effect of frequency offset has not thoroughly been investigated. Since frequency offset degrades the bit error rate (BER) and the quality of channel estimation, its impact cannot be ignored in this case. Moreover, for the AF OFDM case, the convolution of the $S \to R$ and $R \to D$ channels yields the non-Gaussian $S \to R \to D$ channel. Thus, optimal pilot design for cooperative OFDM networks in the presence of frequency offsets is important but currently not available.

Optimal channel estimation is, thus, developed for a cooperative AF or DF OFDM system with frequency offsets. A

two-time-slot cooperative channel estimation protocol is proposed. The source broadcasts the training sequence to the relays and the destination (first time slot), and the relays retransmit the training sequence (second time slot). Pilot designs for AF and DF relays are derived. These new designs eliminate interrelay interference (IRI), which occurs due to the simultaneous relay retransmissions, and minimize the mean square error (MSE). It is proved that to eliminate the IRI, the number of AF and DF relays must be less than $\lfloor N/(2L-1) \rfloor$ and $\lfloor N/L \rfloor$, respectively, where $N$ is the total number of subcarriers, $L$ is the channel order, and $\lfloor a \rfloor$ is the maximum integer part of $a$. The pairwise error probability (PEP) of orthogonal space–time coding in cooperative OFDM due to both frequency offset and channel-estimation errors is also evaluated. The optimal power allocation ratio between the source and the set of relays to minimize the PEP is derived for the two relaying modes.

This paper is organized as follows. Section II introduces the cooperative OFDM system. Channel estimation is developed in Section III. The PEP of the orthogonal space–time-coded system is derived in Section IV. Section V discusses the numerical results. Finally, Section VI concludes this paper.

*Notation:* $(\cdot)^T$, $(\cdot)^H$, $(\cdot)^{-1}$, and $(\cdot)^*$ denote the transpose, conjugate transpose, inverse, and complex conjugate, respectively. The imaginary unit is $\jmath = \sqrt{-1}$. A circularly symmetric complex Gaussian variable with mean $a$ and variance $\sigma^2$ is denoted by $z \sim \mathcal{CN}(a, \sigma^2)$. The $N \times N$ identity matrix is $\mathbf{I}_N$. The $M \times N$ all-zero matrix is $\mathbf{O}_{M \times N}$, and the $N \times 1$ all-zero vector is $\mathbf{0}_N$. The diagonal matrix $\mathrm{diag}\{\mathbf{x}\}$ has the $n$th diagonal element $\mathbf{x}[n]$. The mean and the variance are $\mathbb{E}\{\bullet\}$ and $\mathrm{Var}\{\bullet\}$, respectively.

## II. COOPERATIVE OFDM SIGNAL MODEL

### A. Channel Model

We consider a network with source $(S)$, $k$th relay $R_k$, $k \in \{1, \ldots, M\}$, and destination $(D)$. The time-invariant composite channel impulse response between any pair of nodes $a$ and $b$ is modeled as $h_{a,b}(\tau) = \sum_{l=0}^{L-1} h_{a,b}[l]\delta(\tau - lT_s)$, where $h_{a,b}[l]$ is the $l$th channel gain, and $\delta(x)$ is the unit impulse function. The delays are $\{0, T_s, 2T_s, \ldots, (L-1)T_s\}$. $L$ is the channel order, and $T_s = 1/B$, where $B$ represents the total bandwidth. The channel order $L$ is the same for any pair of nodes. For brevity, we define $\tilde{\mathbf{h}}_{a,b} = [h_{a,b}(0), h_{a,b}(1), \ldots, h_{a,b}(L-1)]^T$. The frequency-domain channel coefficient matrix is $\mathbf{H}_{a,b} = \mathrm{diag}\{H_{a,b}[0], \ldots, H_{a,b}[N-1]\}$, where $H_{a,b}[n] = \sum_{d=0}^{L-1} h_{a,b}(d)e^{-(\jmath 2\pi nd/N)}$ is the channel frequency response on the $n$th subcarrier.

The channel gains $h_{a,b}(l)$ are modeled as complex Gaussian zero-mean random variables (RVs). The channel total power profile for each $S \rightarrow R_k$ channel is normalized. Both $S \rightarrow D$ and $R_k \rightarrow D$ channels suffer large-scale and small-scale fading. The distance between $S$ and $R_k$ is much smaller than that between $S$ and $D$ or that between $R_k$ and $D$. Thus, an identical large-scale fading coefficient $\mathcal{L}_u$ is used for each $S \rightarrow D$ or $R_k \rightarrow D$ channel.[1]

### B. OFDM Signal Model

The input data bits are first mapped to the complex symbols drawn from a signal constellation such as phase-shift keying (PSK) or quadrature amplitude modulation (QAM). The node $S$ transmits the symbol vector $\tilde{\mathbf{X}}_S = [X_S[0], X_S[1], \ldots, X_S[N-1]]^T$, where $N$ is the number of subcarriers. This signal $\tilde{\mathbf{X}}_S$ can be decomposed as $\tilde{\mathbf{X}}_S = \tilde{\mathbf{X}}_S^d + \tilde{\mathbf{X}}_S^p$, where $\tilde{\mathbf{X}}_S^d$ and $\tilde{\mathbf{X}}_S^p$ are $N \times 1$ data and pilot vectors. Data entries of $\tilde{\mathbf{X}}_S$, i.e., PSK or QAM symbols, are modeled as zero-mean and unit-variance RVs. In general, a total of $\mathcal{N}_p$ pilots are allocated per symbol. Therefore, $\tilde{\mathbf{X}}_S^p$ is nonzero only at locations $(\theta_1, \ldots, \theta_{\mathcal{N}_p})$, where $0 \leq \theta_1 < \cdots < \theta_{\mathcal{N}_p} \leq N - 1$. During channel estimation, the whole frame is only occupied by pilots, i.e., $\mathcal{N}_p = N$ and $\tilde{\mathbf{X}}_S^d = \mathbf{0}_N$.

### C. First Time Slot (Preamble Period)

The received samples at the destination $D$ and the $k$th relay $R_k$ are given by

$$y_{D,1}(n) = \sqrt{\frac{\alpha \bar{P}}{N}} \sum_{i=0}^{N-1} X_S[i] H_{D,S}[i] e^{\frac{\jmath 2\pi n(i+\varepsilon_{D,S})}{N}} + w_{D,1}(n) \tag{1a}$$

$$y_{R_k,1}(n) = \sqrt{\frac{\alpha \bar{P}}{N}} \sum_{i=0}^{N-1} X_S[i] H_{R_k,S}[i] e^{\frac{\jmath 2\pi n(i+\varepsilon_{R_k,S})}{N}} + w_{R_k}(n) \tag{1b}$$

where $n = 0, 1, \ldots, N-1$, $\alpha$ is the power allocation ratio between $S$ and the set of relays ($0 < \alpha < 1$), $\bar{P}$ is the average power of each subcarrier,[2] $\varepsilon_{b,S}$ is the normalized frequency offset between nodes $S$ and $b (b \in \{R_k, D\})$, and $w_{D,1}(n)$ and $w_{R_k}(n)$ are the additive white Gaussian noise (AWGN) samples with $\{w_{D,1}(n), w_{R_k}(n)\} \sim \mathcal{CN}(0, \sigma_w^2)$.

The received samples at $D$ and $R_k$ are $\mathbf{y}_{D,1} = [y_{D,1}(0), y_{D,1}(1), \ldots, y_{D,1}(N-1)]^T$ and $\mathbf{y}_{R_k,1} = [y_{R_k,1}(0), y_{R_k,1}(1), \ldots, y_{R_k,1}(N-1)]^T$. The post discrete Fourier transform (DFT) demodulator outputs are then

$$\begin{aligned}
\mathbf{r}_{D,1} &= \mathbf{F}^H \mathbf{y}_{D,1} \\
&= \underbrace{\sqrt{\alpha N \bar{P}} \mathbf{E}_{D,S}^{\mathrm{cir}} \mathbf{X}_S^p \mathbf{F}_{(L)}^H \tilde{\mathbf{h}}_{D,S}}_{\mathbf{P}_{D,S} \ (N \times L)} \\
&\quad + \underbrace{\sqrt{\alpha N \bar{P}} \mathbf{E}_{D,S}^{\mathrm{cir}} \mathbf{X}_S^d \mathbf{F}_{(L)}^H \tilde{\mathbf{h}}_{D,S}}_{\text{Interference}} + \underbrace{\mathbf{F}^H \mathbf{w}_{D,1}}_{\boldsymbol{\eta}_{D,1} \ (N \times 1)}
\end{aligned} \tag{2a}$$

$$\begin{aligned}
\mathbf{r}_{R_k,1} &= \mathbf{F}^H \mathbf{y}_{R_k,1} \\
&= \underbrace{\sqrt{\alpha N \bar{P}} \mathbf{E}_{R_k,S}^{\mathrm{cir}} \mathbf{X}_S^p \mathbf{F}_{(L)}^H \tilde{\mathbf{h}}_{R_k,S}}_{\mathbf{P}_{R_k,S} \ (N \times L)} \\
&\quad + \underbrace{\sqrt{\alpha N \bar{P}} \mathbf{E}_{R_k,S}^{\mathrm{cir}} \mathbf{X}_S^d \mathbf{F}_{(L)}^H \tilde{\mathbf{h}}_{R_k,S}}_{\text{Interference}} + \underbrace{\mathbf{F}^H \mathbf{w}_{R_k}}_{\boldsymbol{\eta}_{R_k,1} \ (N \times 1)}
\end{aligned} \tag{2b}$$

where $\mathbf{w}_{D,1} = [w_{D,1}(0), w_{D,1}(1), \ldots, w_{D,1}(N-1)]^T$, $\mathbf{w}_{R_k} = [w_{R_k}(0), w_{R_k}(1), \ldots, w_{R_k}(N-1)]^T$, and the inverse DFT

---

[1]The large-scale fading coefficient $\mathcal{L}_u$ can be approximated as $\mathcal{L}_u = d_{D,S}^{-q}/2$ (or $\mathcal{L}_u = d_{D,R}^{-q}/2$), where $d_{a,b}$ represents the distance between nodes $a$ and $b$, and $2 \leq q \leq 6$ [26].

[2]Identical power is allocated to each subcarrier, regardless of the pilot or data subcarrier.

(IDFT) matrix $\mathbf{F}$ is defined as $[\mathbf{F}]_{nk} = (1/\sqrt{N})e^{(J2\pi nk/N)}$ for $0 \le (n,k) \le N-1$. The frequency-offset-dependent matrix $\mathbf{E}_{a,b}$ is defined by $\mathbf{E}_{a,b} = \mathrm{diag}\{1, e^{(J2\pi\varepsilon_{a,b}/N)}, \ldots,$ $e^{(J2\pi\varepsilon_{a,b}(N-1)/N)}\}$. $\mathbf{E}_{a,b}^{\mathrm{cir}} = \mathbf{F}^H \mathbf{E}_{a,b}\mathbf{F}$. $\mathbf{F}_{(L)}$ is the first $L$ rows of $\mathbf{F}$, and $\mathbf{X}_S = \mathbf{X}_S^d + \mathbf{X}_S^p$ is an $N \times N$ diagonal matrix with $\mathbf{X}_S^d = \mathrm{diag}\{\tilde{\mathbf{X}}_S^d\}$ and $\mathbf{X}_S^p = \mathrm{diag}\{\tilde{\mathbf{X}}_S^p\}$.

### D. Second Time Slot

The relays retransmit the received signal to $D$. The total power equally allocated to all the relays is $(1-\alpha)N\bar{P}$.

*1) AF Mode:* In this case, each relay simply retransmits the received signal to the destination. The received symbol at $D$ is $\mathbf{y}_{D,2}^{\mathrm{AF}} = \rho_R\sqrt{((1-\alpha)\bar{P}/M)}\sum_{k=1}^{M}\mathbf{E}_{D,R_k}\mathbf{FH}_{D,R_k}\mathbf{r}_{R_k,1} + \mathbf{w}_{D,2}$, where $\rho_R = (\alpha\bar{P} + \sigma_w^2)^{-(1/2)}$ represents the amplifying coefficients at each relay. The received signal at the destination $D$ can be demodulated as

$$
\begin{aligned}
\mathbf{r}_{D,2}^{\mathrm{AF}} &= \mathbf{F}^H \mathbf{y}_{D,2}^{\mathrm{AF}} \\
&= \mathbf{F}^H \rho_R \sqrt{\frac{(1-\alpha)\bar{P}}{M}}\sum_{k=1}^{M}\mathbf{E}_{D,R_k}\mathbf{FH}_{D,R_k}\mathbf{r}_{R_k,1} + \mathbf{F}^H\mathbf{w}_{D,2} \\
&= \frac{Q_2(\alpha)}{\sqrt{N}}\sum_{k=1}^{M}\mathbf{F}^H\mathbf{E}_{D,R_k}\mathbf{FH}_{D,R_k}\mathbf{r}_{R_k,1} + \mathbf{F}^H\mathbf{w}_{D,2} \\
&= Q_1(\alpha)\sum_{k=1}^{M}\overbrace{\mathbf{F}^H\underbrace{\mathbf{E}_{D,R_k}\mathbf{E}_{R_k,S}}_{=\mathbf{E}_{D,R_k,S}}\mathbf{F}}^{=\mathbf{E}_{D,R_k,S}^{\mathrm{cir}}}\mathbf{H}_{R_k,S}\mathbf{H}_{D,R_k}\tilde{\mathbf{X}}_S^p \\
&\quad + Q_1(\alpha)\sum_{k=1}^{M}\mathbf{E}_{D,R_k,S}^{\mathrm{cir}}\mathbf{H}_{R_k,S}\mathbf{H}_{D,R_k}\tilde{\mathbf{X}}_S^d \\
&\quad + \frac{Q_2(\alpha)}{\sqrt{N}}\sum_{k=1}^{M}\mathbf{E}_{D,R_k}^{\mathrm{cir}}\mathbf{H}_{D,R_k}\mathbf{F}^H\mathbf{w}_{R_k} + \mathbf{F}^H\mathbf{w}_{D,2} \\
&= Q_1(\alpha)\sum_{k=1}^{M}\mathbf{E}_{D,R_k,S}^{\mathrm{cir}}(\mathbf{X}_S^p + \mathbf{X}_S^d) \\
&\quad \cdot \mathbf{F}_{(2L-1)}^H\left(\tilde{\mathbf{h}}_{R_k,S}^T \otimes \tilde{\mathbf{h}}_{D,R_k}^T\right)^T \\
&\quad + \frac{Q_2(\alpha)}{\sqrt{N}}\sum_{k=1}^{M}\mathbf{E}_{D,R_k}^{\mathrm{cir}}\mathbf{H}_{D,R_k}\mathbf{F}^H\mathbf{w}_{R_k} + \mathbf{F}^H\mathbf{w}_{D,2} \quad (3)
\end{aligned}
$$

where $Q_1(\alpha) = \sqrt{\alpha(1-\alpha)N\bar{P}^2/M(\alpha\bar{P}+\sigma_w^2)}$, $Q_2(\alpha) = \sqrt{(1-\alpha)N\bar{P}/M(\alpha\bar{P}+\sigma_w^2)}$, $\mathbf{E}_{D,R_k,S}^{\mathrm{cir}} = \mathbf{F}^H\mathbf{E}_{D,R_k}\mathbf{E}_{R_k,S}\mathbf{F} = \mathbf{E}_{D,S}^{\mathrm{cir}}$, $\mathbf{W}_\eta = \mathrm{diag}\{\boldsymbol{\eta}_{R_k,1}\}$, $\tilde{\mathbf{h}}_{D,R_k,S} = (\tilde{\mathbf{h}}_{R_k,S}^T \otimes \tilde{\mathbf{h}}_{D,R_k}^T)^T$, and $\otimes$ denotes convolution. Equation (3) can further be simplified as

$$
\begin{aligned}
\mathbf{r}_{D,2}^{\mathrm{AF}} &= \sum_{k=1}^{M}Q_1(\alpha)\mathbf{E}_{D,R_k,S}^{\mathrm{cir}}\mathbf{X}_S^d\mathbf{F}_{(2L-1)}^H\tilde{\mathbf{h}}_{D,R_k,S} \\
&\quad + \sum_{k=1}^{M}\underbrace{Q_1(\alpha)\mathbf{E}_{D,R_k,S}^{\mathrm{cir}}\mathbf{X}_S^p\mathbf{F}_{(2L-1)}^H}_{\mathbf{P}_{D,R_k,S}^{\mathrm{AF}}\ (N\times(2L-1))}\tilde{\mathbf{h}}_{D,R_k,S} \\
&\quad + \underbrace{\sum_{k=1}^{M}Q_2(\alpha)\mathbf{E}_{D,R_k}^{\mathrm{cir}}\mathbf{W}_\eta\mathbf{F}_{(L)}^H\tilde{\mathbf{h}}_{D,R_k} + \mathbf{F}^H\mathbf{w}_{D,2}}_{\boldsymbol{\eta}_{D,2}^{\mathrm{AF}}}. \quad (4)
\end{aligned}
$$

*2) DF Mode:* Each DF relay decodes and reencodes the received signal. Unlike the AF mode, the DF mode can eliminate the additive noise and interference that accumulated in the relays. It is assumed that $m$ out of $M$ relays can correctly decode,[3] and the received symbol at node $D$ is $\mathbf{y}_{D,2}^{\mathrm{DF}} = \sqrt{(1-\alpha)\bar{P}/m}\sum_{k=1}^{m}\mathbf{E}_{D,R_k}\mathbf{FH}_{D,R_k}\tilde{\mathbf{X}}_{R_k} + \mathbf{w}_{D,2}$. The post-DFT output of $\mathbf{y}_{D,2}^{\mathrm{DF}}$ is

$$
\begin{aligned}
\mathbf{r}_{D,2}^{\mathrm{DF}} &= \mathbf{F}^H \mathbf{y}_{D,2}^{\mathrm{DF}} \\
&= \sum_{k=1}^{m}\sqrt{\frac{(1-\alpha)N\bar{P}}{m}}\mathbf{E}_{D,R_k}^{\mathrm{cir}}\mathbf{X}_{R_k}^d\mathbf{F}_{(L)}^H\tilde{\mathbf{h}}_{D,R_k} \\
&\quad + \sum_{k=1}^{m}\underbrace{\sqrt{\frac{(1-\alpha)N\bar{P}}{m}}\mathbf{E}_{D,R_k}^{\mathrm{cir}}\mathbf{X}_{R_k}^p\mathbf{F}_{(L)}^H}_{\mathbf{P}_{D,R_k}^{\mathrm{DF}}\ (N\times L)}\tilde{\mathbf{h}}_{D,R_k} + \underbrace{\mathbf{F}^H\mathbf{w}_{D,2}}_{\boldsymbol{\eta}_{D,2}^{\mathrm{DF}}}.
\end{aligned}
$$
$$\text{(5)}$$

A transceiver system model diagram for the proposed cooperative transmission is illustrated in Fig. 1, where the cooperation is performed in two time slots, and transceivers for both AF and DF relaying modes are given out.

### III. CHANNEL ESTIMATION

Channel estimation for the cooperative OFDM uplink is developed next. Since $D$ receives from $S$ only in the first time slot, conventional least-square (LS) estimation is possible. However, in the second time slot, $D$ receives multiple simultaneous relay transmissions, which results in IRI.

### A. Channel Estimation in the First Time Slot

From (2), the LS estimation of the $S \to D$ channel response $\tilde{\mathbf{h}}_{D,S}$ is given by $\hat{\tilde{\mathbf{h}}}_{D,S} = \mathbf{P}_{D,S}^\dagger\mathbf{r}_{D,1}$, where $\mathbf{P}_{D,S}^\dagger = (\mathbf{P}_{D,S}^H\mathbf{P}_{D,S})^{-1}\mathbf{P}_{D,S}^H$. The MSE of $\hat{\tilde{\mathbf{h}}}_{D,S}$ is obtained as $\mathrm{MSE}(\hat{\tilde{\mathbf{h}}}_{D,S}) = (1/L)\mathbb{E}\{\|\hat{\tilde{\mathbf{h}}}_{D,S} - \tilde{\mathbf{h}}_{D,S}\|_2^2\}$. Similarly, that for the $S \to R_k$ channel response is $\mathrm{MSE}(\hat{\tilde{\mathbf{h}}}_{R_k,S}) = (1/L)\mathbb{E}\{\|\hat{\tilde{\mathbf{h}}}_{R_k,S} - \tilde{\mathbf{h}}_{R_k,S}\|_2^2\}$.

### B. Pilot Design to Eliminate IRI in the Second Time Slot

Since an identical pilot, i.e., $\mathbf{X}_S^p$, is received at each relay in the first time slot, the received pilot at the destination $D$ in the second time slot is also $\mathbf{X}_S^p$ if the relays simply retransmit the received signal without modifying it. In this case, $D$ does not know where the received pilots come from, and therefore, it cannot identify $\tilde{\mathbf{h}}_{D,R_k,S}$ in the AF mode (or $\tilde{\mathbf{h}}_{D,R_k}$ in the DF mode).

With multiple relay transmissions, the IRI must be eliminated to minimize the MSE. An optimal pilot design in MIMO-OFDM systems in the presence of frequency offsets is discussed in [22], and the proposed pilots can readily be adapted

---

[3]Error correction codes, e.g., cyclic redundancy check (CRC) bits, may be required. This is beyond the scope of this paper.
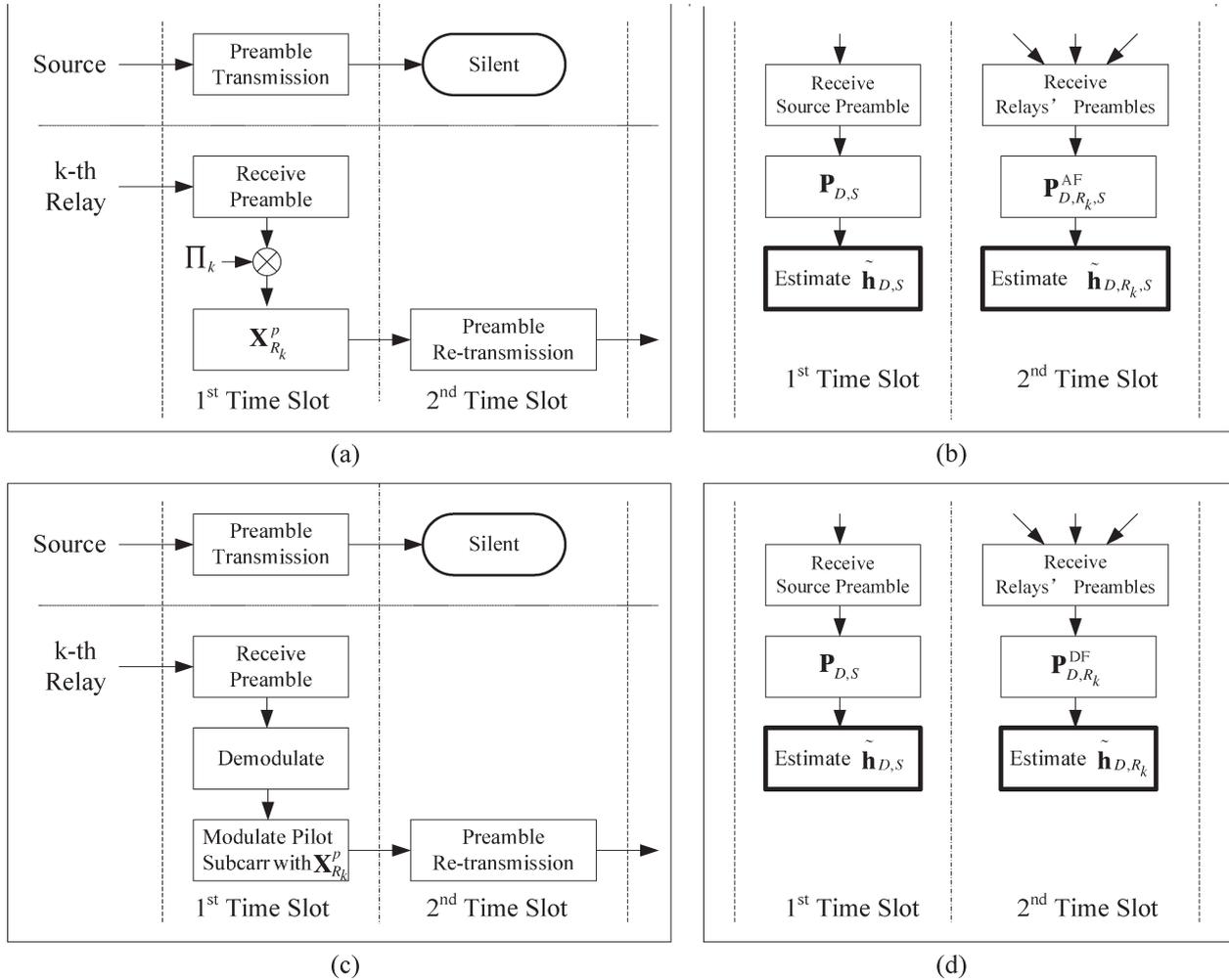
Fig. 1.   Transceiver system model diagram for the proposed cooperative transmission. (a) Transmitter in AF mode. (b) Receiver in AF mode. (c) Transmitter in DF mode. (d) Receiver in DF mode.

here. The retransmitted pilot for the relay $R_k$ is $\mathbf{X}^p_{R_k}$. The IRI between different relays can be eliminated if

$$\left(\mathbf{P}^{\text{AF}}_{D,R_k,S}\right)^{\dagger} \mathbf{P}^{\text{AF}}_{D,R_i,S} = \mathbf{O}_{(2L-1)\times(2L-1)} \quad \text{(AF Mode)} \quad (6a)$$

$$\left(\mathbf{P}^{\text{DF}}_{D,R_k}\right)^{\dagger} \mathbf{P}^{\text{DF}}_{D,R_i} = \mathbf{O}_{L\times L} \quad \text{(DF Mode)} \quad (6b)$$

is satisfied for each $i \neq k$. In DF mode, (6) can easily be satisfied by modulating different pilots in different relays before their retransmission. However, in AF mode, (6) cannot be satisfied unless each relay modifies its received pilot.

*1) AF Mode:* A modified AF relaying mode is applied in each relay to satisfy (6). The $k$th relay $R_k$ multiplies its received signal $\mathbf{y}_{R_k,1}$ by a premodulation matrix $\mathbf{\Pi}_k$ and retransmits. The received signal at $D$ can then be demodulated as

$$\tilde{\mathbf{r}}^{\text{AF}}_{D,2} = \mathbf{F}^H \sum_{k=1}^{M} \mathbf{E}_{D,R_k} \mathbf{F} \mathbf{\Pi}_k \mathbf{y}_{R_k,1} \quad (7)$$

and it can further be resolved as

$$\tilde{\mathbf{r}}^{\text{AF}}_{D,2} = \sum_{k=1}^{M} Q_1(\alpha) \mathbf{E}^{\text{cir}}_{D,R_k} \mathbf{\Pi}_k \mathbf{E}^{\text{cir}}_{R_k,S} \mathbf{X}^d_S \mathbf{F}^H_{(2L-1)} \tilde{\mathbf{h}}_{D,R_k,S}$$

$$+ \sum_{k=1}^{M} Q_1(\alpha) \underbrace{\mathbf{E}^{\text{cir}}_{D,R_k} \mathbf{\Pi}_k \mathbf{E}^{\text{cir}}_{R_k,S} \mathbf{X}^p_S}_{=\mathbf{E}^{\text{cir}}_{D,S} \mathbf{X}^p_{R_k}} \mathbf{F}^H_{(2L-1)} \tilde{\mathbf{h}}_{D,R_k,S}$$

$$\underbrace{\qquad\qquad\qquad\qquad}_{\tilde{\mathbf{P}}^{\text{AF}}_{D,R_k,S}}$$

$$+ \underbrace{\sum_{k=1}^{M} Q_2(\alpha) \mathbf{E}^{\text{cir}}_{D,R_k} \mathbf{\Pi}_k \mathbf{W}_\eta \mathbf{F}^H_{(L)} \tilde{\mathbf{h}}_{D,R_k} + \mathbf{F}^H \mathbf{w}_{D,2}}_{\tilde{\boldsymbol{\eta}}^{\text{AF}}_{D,2}} \quad (8)$$

where $\mathbf{X}^p_{R_k}$ is a unique pilot of $R_k$ and different from $\mathbf{X}^p_S$.[4] Equation (8) can be understood as each relay uses a unique premodulation matrix $\mathbf{\Pi}_k$ to do some modification to its pilot subcarriers (how to obtain $\mathbf{\Pi}_k$ will be discussed later). The LS channel estimation[5] is $\hat{\mathbf{h}}_{DRS} = (\mathbf{P}^{\text{AF}}_2)^{\dagger}\tilde{\mathbf{r}}^{\text{AF}}_{D,2}$, where

---

[4]In the following analysis, we assume that a unique pilot is allocated to each node, and $D$ knows pilot of each mobile node. A pilot-allocation scheme should be performed to mitigate the collision among pilots of different relays, but how to perform this pilot allocation scheme is beyond the scope of this paper. An example of pilot allocation is given in [22].

[5]Since the relay channel in the AF mode is no longer Gaussian, the proposed LS channel estimator is not minimum-variance unbiased (MVU) estimator, and it cannot be called "optimal." However, in DF mode, the $R \to D$ channel is Gaussian, and the proposed LS estimator is the MVU estimator.

$\mathbf{P}_2^{\text{AF}} = [\tilde{\mathbf{P}}_{D,R_1,S}^{\text{AF}} \quad \cdots \quad \tilde{\mathbf{P}}_{D,R_M,S}^{\text{AF}}]$, and $\mathbf{h}_{DRS} = [\tilde{\mathbf{h}}_{D,R_1,S}^T, \ldots,$ $\tilde{\mathbf{h}}_{D,R_M,S}^T]^T$. In this paper, all the pilots are modulated in one symbol, and the pilot subcarriers are shared by all the nodes. The pilots that satisfy (6) for the $k$th node in the AF mode is resolved as

$$\left[\mathbf{X}_{R_k}^p\right]_{\theta_i\theta_i} = e^{\frac{j2\pi\theta_i(k-1)(2L-1)}{N}}$$
$$k = 1, \ldots, M; \quad i = 1, \ldots, \mathcal{N}_p$$

$$\text{s.t.} \quad (2L-1)M \leq \mathcal{N}_p \leq N, \quad \frac{N}{\mathcal{N}_p} = \text{integer}$$

$$\frac{\theta_i(k-l)(2L-1)}{N} \neq \text{integer}, \qquad k \neq l$$

$$\theta_2 - \theta_1 = \theta_3 - \theta_2 = \cdots = \theta_{\mathcal{N}_p} - \theta_{\mathcal{N}_p-1} = \frac{N}{\mathcal{N}_p}. \quad (9)$$

By using the pilot defined in (9), the MSE of $\hat{\mathbf{h}}_{DRS}$ is given by

$$\text{MSE}(\hat{\mathbf{h}}_{DRS}) = \frac{1}{(2L-1)M}\mathbb{E}\left\{\|\hat{\mathbf{h}}_{DRS} - \mathbf{h}_{DRS}\|_2^2\right\}$$
$$= \frac{(N - \mathcal{N}_p) \cdot \text{trace}\left\{\mathbf{\Phi}_2^{\text{AF}}\right\}}{\mathcal{N}_p(2L-1)M}$$
$$+ \frac{\sigma_w^2 \sum_{k=1}^M \text{trace}\{\mathbf{\Phi}_{D,R_k}^{\text{AF}}\}}{\alpha\mathcal{N}_p(2L-1)M\bar{P}} + \frac{M(\alpha\bar{P} + \sigma_w^2)\sigma_w^2}{\alpha(1-\alpha)\mathcal{N}_p\bar{P}^2}$$
$$(10)$$

where $\mathbf{\Phi}_2^{\text{AF}} = \mathbb{E}\{\mathbf{h}_{DRS}\mathbf{h}_{DRS}^H\}$, and $\mathbf{\Phi}_{D,R_k}^{\text{AF}} = \mathbb{E}\{\tilde{\mathbf{h}}_{D,R_k}\tilde{\mathbf{h}}_{D,R_k}^H\}$.

We will now derive $\mathbf{\Pi}_k$ to satisfy $\mathbf{E}_{D,R_k}^{\text{cir}}\mathbf{\Pi}_k\mathbf{E}_{R_k,S}^{\text{cir}}\mathbf{X}_S^p = \mathbf{E}_{D,S}^{\text{cir}}\mathbf{X}_{R_k}^p$. Without loss of generality, we assume that the pilot with $m = 1$ is allocated to $S$ and that $\mathbf{X}_{R_k}^p$ can be represented as $\mathbf{X}_{R_k}^p = \mathbf{\Lambda}_k\mathbf{X}_S^p$, where $\mathbf{\Lambda}_k$ is a diagonal matrix with $[\mathbf{\Lambda}_k]_{\theta_i\theta_i} = e^{(j2\pi\theta_i(k-1)(2L-1)/N)}$, and $[\mathbf{\Lambda}_k]_{ll} = 0$ for each $l \neq \theta_i$. Note that $\mathbf{E}_{D,S}^{\text{cir}} = \mathbf{E}_{D,R_k}^{\text{cir}}\mathbf{E}_{R_k,S}^{\text{cir}}$ is satisfied for each $k$, so the problem is reduced to finding $\mathbf{\Pi}_k$ to make $\mathbf{\Pi}_k\mathbf{E}_{R_k,S}^{\text{cir}} = \mathbf{E}_{R_k,S}^{\text{cir}}\mathbf{\Lambda}_k$, which is resolved as

$$\mathbf{\Pi}_k = \mathbf{E}_{R_k,S}^{\text{cir}}\mathbf{\Lambda}_k(\mathbf{E}_{R_k,S}^{\text{cir}})^{-1}$$
$$= \mathbf{F}^H\mathbf{E}_{R_k,S}\mathbf{F}\mathbf{\Lambda}_k\mathbf{F}^H\mathbf{E}_{R_k,S}^{-1}\mathbf{F}. \quad (11)$$

Since $\mathbf{\Pi}_k$ modifies only the pilot subcarriers by performing a phase rotation to the received pilots at $R_k$, the data subcarriers remain unaffected.

Note that the pilot given in (9) eliminates the IRI only when the number of relays does not exceed a specified value. The following lemma provides the maximum number of relays in the AF mode.

*Lemma 1—Maximum Number of Relays in the AF Mode:* In AF mode, to minimize the variance error of the LS estimator for each $S \rightarrow R \rightarrow D$ channel, the maximum number of active relays that simultaneously retransmit is $M \leq \lfloor N/(2L-1) \rfloor$.

*Proof:* In AF mode, the channel order for all the $S \rightarrow R \rightarrow D$ channels is $2L-1$. From (9), the condition of $(2L-1)M \leq \mathcal{N}_p \leq N$ must be satisfied for the pilot design, and consequently, $M \leq \lfloor(N/2L-1)\rfloor$. ∎

Lemma 1 indicates that the maximum number of active relays is inversely proportional to $2L-1$. Since the achievable

cooperative diversity gain is proportional to the number of relays, this condition describes a tradeoff between the channel estimation ability and the achievable diversity gain.

*2) DF Mode:* Each active relay retransmits in the second time slot by modulating the pilot subcarriers with its own pilot but without changing the data subcarriers. The LS channel estimate is then given by $\hat{\mathbf{h}}_{DR} = (\mathbf{P}_2^{\text{DF}})^\dagger\mathbf{r}_{D,2}^{\text{DF}}$, where $\mathbf{P}_2^{\text{DF}} = [\mathbf{P}_{D,R_1}^{\text{DF}} \quad \cdots \quad \mathbf{P}_{D,R_m}^{\text{DF}}]$, and $\mathbf{h}_{DR} = [\tilde{\mathbf{h}}_{D,R_1}^T, \ldots, \tilde{\mathbf{h}}_{D,R_m}^T]^T$.

The optimal pilot for $R_k$ in DF mode is given by

$$\left[\mathbf{X}_{R_k}^p\right]_{\theta_i\theta_i} = e^{\frac{j2\pi\theta_i(k-1)L}{N}}$$
$$k = 1, \ldots, M; \quad i = 1, \ldots, \mathcal{N}_p$$

$$\text{s.t.} \quad LM \leq \mathcal{N}_p \leq N, \quad \frac{N}{\mathcal{N}_p} = \text{integer}$$

$$\frac{\theta_i(k-l)L}{N} \neq \text{integer}, \qquad k \neq l$$

$$\theta_2 - \theta_1 = \theta_3 - \theta_2 = \cdots = \theta_{\mathcal{N}_p} - \theta_{\mathcal{N}_p-1} = \frac{N}{\mathcal{N}_p}. \quad (12)$$

By using (12), the MSE of $\hat{\mathbf{h}}_{DR}$ is

$$\text{MSE}(\hat{\mathbf{h}}_{DR}) = \frac{1}{Lm}\mathbb{E}\left\{\|\hat{\mathbf{h}}_{DR} - \mathbf{h}_{DR}\|_2^2\right\}$$
$$= \frac{N - \mathcal{N}_p}{\mathcal{N}_p} \cdot \frac{\text{trace}\left\{\mathbf{\Phi}_2^{\text{DF}}\right\}}{Lm} + \frac{m\sigma_w^2}{(1-\alpha)\mathcal{N}_p\bar{P}} \quad (13)$$

where $\mathbf{\Phi}_2^{\text{DF}} = \mathbb{E}\{\mathbf{h}_{DR}\mathbf{h}_{DR}^H\}$.

As with the AF mode, the maximum number of DF relays is constrained. The following lemma provides this maximum number.

*Lemma 2—Maximum Number of Relays in the DF Mode:* In DF mode, to achieve the optimal LS channel estimation for each $S \rightarrow R \rightarrow D$ channel, the maximum number of active relays that simultaneously retransmit is $M \leq \lfloor N/L \rfloor$.

*Proof:* In DF mode, the channel order for each $R \rightarrow D$ channel is $L$. From (12), the condition of $LM \leq \mathcal{N}_p \leq N$ must be satisfied for optimal pilot design, and we can easily conclude that $M \leq \lfloor N/L \rfloor$. ∎

### C. Effect of Imperfect Frequency Offset Estimation on Channel Estimation

Up to now, a perfect frequency offset knowledge is assumed. However, this section considers the frequency offset errors. We use $e_{a,b}$ to represent the estimation error of $\varepsilon_{a,b}$.[6] At node $D$, $\mathbf{E}_{D,z}, z = \{S, R_k\}$ can be estimated as

$$\hat{\mathbf{E}}_{D,z} = \text{diag}\left\{1, e^{\frac{j2\pi\hat{\varepsilon}_{D,z}}{N}}, \ldots, e^{\frac{j2\pi(N-1)\hat{\varepsilon}_{D,z}}{N}}\right\}$$
$$\underbrace{\qquad\qquad\qquad}_{\Delta\mathbf{E}_{D,z}}$$
$$\cong \mathbf{E}_{D,z} + \overbrace{je_{D,z} \cdot \text{diag}\left\{0, \frac{2\pi}{N}, \ldots, \frac{2\pi(N-1)}{N}\right\}}^{\mathbf{\Omega}} \cdot \mathbf{E}_{D,z}.$$
$$(14)$$

---

[6]An identical variance error of the frequency offset estimation, i.e., $\sigma_e^2$, is assumed in each node. Although the frequency offset estimation errors in different nodes are usually different (see [27]), the difference among them is negligible at high SINR.

Using $\hat{\mathbf{P}}_{D,S}$, $\hat{\mathbf{P}}_2^{\text{AF}}$, and $\hat{\mathbf{P}}_2^{\text{DF}}$ to represent the estimated $\mathbf{P}_{D,S}$, $\mathbf{P}_2^{\text{AF}}$, and $\mathbf{P}_2^{\text{DF}}$, respectively, we have

$$\hat{\mathbf{P}}_{D,S} = \sqrt{\alpha N\bar{P}}\hat{\mathbf{E}}_{D,S}^{\text{cir}}\mathbf{X}_S^p\mathbf{F}_{(L)}^H$$
$$= \underbrace{\sqrt{\alpha N\bar{P}}\mathbf{E}_{D,S}^{\text{cir}}\mathbf{X}_S^p\mathbf{F}_{(L)}^H}_{\mathbf{P}_{D,S}} + \underbrace{\sqrt{\alpha N\bar{P}}\Delta\mathbf{E}_{D,S}^{\text{cir}}\mathbf{X}_S^p\mathbf{F}_{(L)}^H}_{\Delta\mathbf{P}_{D,S}} \quad (15)$$

$$\hat{\mathbf{P}}_2^{\text{AF}} = \mathbf{P}_2^{\text{AF}} + \underbrace{Q_1(\alpha)\mathbf{F}^H\Delta\mathbf{E}_{D,S}\mathbf{F}[\mathbf{X}_{R_1}^p \cdots \mathbf{X}_{R_M}^p]\mathbf{F}_{(2L-1)}^H}_{\Delta\mathbf{P}_2^{\text{AF}}} \quad (16)$$

$$\hat{\mathbf{P}}_2^{\text{DF}} = \mathbf{P}_2^{\text{DF}} + \underbrace{\sqrt{\frac{(1-\alpha)N\bar{P}}{m}}\mathbf{F}^H\Delta_2^{\text{DF}}\mathbf{F}_{(L)}^H}_{\Delta\mathbf{P}_2^{\text{DF}}} \quad (17)$$

where $\Delta_2^{\text{DF}} = [\Delta\mathbf{E}_{D,R_1}\mathbf{F}\mathbf{X}_{R_1}^p \cdots \Delta\mathbf{E}_{D,R_M}\mathbf{F}\mathbf{X}_{R_m}^p]$. We can express $\hat{\mathbf{P}}_{D,S}^{\dagger}$ as

$$\hat{\mathbf{P}}_{D,S}^{\dagger} = \left(\underbrace{\mathbf{P}_{D,S}^H\mathbf{P}_{D,S}}_{=\alpha\bar{P}\mathbf{I}_{\mathcal{N}_p}} + \mathbf{BSB}^H\right)^{-1}(\mathbf{P}_{D,S} + \Delta\mathbf{P}_{D,S})^H$$
$$= \mathbf{P}_{D,S}^{\dagger} + \Delta\mathbf{P}_{D,S}^{\dagger} \quad (18)$$

where $\mathbf{BSB}^H = \Delta\mathbf{P}_{D,S}^H\mathbf{P}_{D,S} + \mathbf{P}_{D,S}^H\Delta\mathbf{P}_{D,S} + \Delta\mathbf{P}_{D,S}^H\Delta\mathbf{P}_{D,S}$, $\Delta\mathbf{P}_{D,S}^{\dagger} = (\mathbf{P}_{D,S}^H\mathbf{P}_{D,S})^{-1}\Delta\mathbf{P}_{D,S}^H - (1/\alpha\bar{P})\mathbf{B}(\mathbf{B}^H\mathbf{B} + \alpha\bar{P}\mathbf{S}^{-1})^{-1}\mathbf{B}^H(\mathbf{P}_{D,S} + \Delta\mathbf{P}_{D,S})^H$, $\mathbf{S} = \text{diag}\{\lambda_0, \lambda_1, \ldots, \lambda_{N-1}\}$, $\lambda_i = (4\pi i e_{D,S}/N)\sin(2\pi i e_{D,S}/N) + (4\pi^2 i^2 e_{D,S}^2/N^2)$, and $\mathbf{B} = \mathbf{F}_{(L)}\mathbf{X}_S^{pH}\mathbf{F}^H$. We also have

$$\mathbf{B}^H\mathbf{B} = \alpha\bar{P}\begin{bmatrix} \mathbf{I}_{\mathcal{N}_p} & \mathbf{O}_{\mathcal{N}_p\times(N-\mathcal{N}_p)} \\ \mathbf{O}_{(N-\mathcal{N}_p)\times\mathcal{N}_p} & \mathbf{O}_{(N-\mathcal{N}_p)\times(N-\mathcal{N}_p)} \end{bmatrix}. \quad (19)$$

From (18) and (19), the matrix $(\mathbf{B}^H\mathbf{B} + \alpha\bar{P}\mathbf{S}^{-1})^{-1}$ must be a diagonal matrix. Using $\tilde{\lambda}_i$ to represent the $i$th eigenvalue of $(\mathbf{B}^H\mathbf{B} + \alpha\bar{P}\mathbf{S}^{-1})^{-1}$, we have

$$\tilde{\lambda}_i = \begin{cases} \frac{\lambda_i}{\alpha\bar{P}(\lambda_i+1)}, & 0 \le i \le \mathcal{N}_p - 1 \\ \frac{\lambda_i}{\alpha\bar{P}}, & \mathcal{N}_p \le i \le N - 1. \end{cases}$$

For small frequency offset errors, $\lambda_i$ can be approximated as $\lambda_i \cong (12\pi^2 i^2 e_{D,S}^2/N^2)$. When $\lambda_i \ll 1$, $\tilde{\lambda}_i \cong \lambda_i$ for each $0 \le i \le N - 1$.

From (18), the first item in $\Delta\mathbf{P}_{D,S}^{\dagger}$ is a function of $e_{D,S}$, but the second item in $\Delta\mathbf{P}_{D,S}^{\dagger}$ is a function of $e_{D,S}^2$. For a small $e_{D,S}$, the second item is negligible as compared with the first item, and $\Delta\mathbf{P}_{D,S}^{\dagger}$ can be approximated as $\Delta\mathbf{P}_{D,S}^{\dagger} \cong (\mathbf{P}_{D,S}^H\mathbf{P}_{D,S})^{-1}\Delta\mathbf{P}_{D,S}^H$ to simplify the analysis. Similarly, we can also represent $(\hat{\mathbf{P}}_2^{\text{AF}})^{\dagger}$ and $(\hat{\mathbf{P}}_2^{\text{DF}})^{\dagger}$ as

$$\left(\hat{\mathbf{P}}_2^{\text{AF}}\right)^{\dagger} \cong \left(\mathbf{P}_2^{\text{AF}}\right)^{\dagger} + \underbrace{\left(\left(\mathbf{P}_2^{\text{AF}}\right)^H\left(\mathbf{P}_2^{\text{AF}}\right)\right)^{-1}\left(\Delta\mathbf{P}_2^{\text{AF}}\right)^H}_{\Delta(\hat{\mathbf{P}}_2^{\text{AF}})^{\dagger}}$$

$$\left(\hat{\mathbf{P}}_2^{\text{DF}}\right)^{\dagger} \cong \left(\mathbf{P}_2^{\text{DF}}\right)^{\dagger} + \underbrace{\left(\left(\mathbf{P}_2^{\text{DF}}\right)^H\left(\mathbf{P}_2^{\text{DF}}\right)\right)^{-1}\left(\Delta\mathbf{P}_2^{\text{DF}}\right)^H}_{\Delta(\hat{\mathbf{P}}_2^{\text{DF}})^{\dagger}}$$

and the LS channel estimation for $\tilde{\mathbf{h}}_{D,S}$, $\tilde{\mathbf{h}}_{R_k,S}$, $\mathbf{h}_{DRS}$, and $\mathbf{h}_{DR}$ are given by $\hat{\tilde{\mathbf{h}}}_{b,S} = \hat{\mathbf{P}}_{b,S}^{\dagger}\mathbf{r}_{b,1}$, $\hat{\mathbf{h}}_{DRS} = (\hat{\mathbf{P}}_2^{\text{AF}})^{\dagger}\tilde{\mathbf{r}}_{D,2}^{\text{AF}}$, and $\hat{\mathbf{h}}_{DR} = (\hat{\mathbf{P}}_2^{\text{DF}})^{\dagger}\mathbf{r}_{D,2}^{\text{DF}}$, respectively, where $b \in \{D, R_k\}$. The MSE of the channel estimation by considering the frequency offset errors can be derived, respectively, as

$$\text{MSE}(\hat{\tilde{\mathbf{h}}}_{b,S})$$
$$= \frac{1}{L}\mathbb{E}\left\{\left\|\hat{\tilde{\mathbf{h}}}_{b,S} - \tilde{\mathbf{h}}_{b,S}\right\|_2^2\right\}$$
$$= \frac{\text{trace}\left\{\left(\mathbf{P}_{b,S}^H\mathbf{P}_{b,S}\right)^{-1}\mathbf{J}_{b,S}\mathbf{\Phi}_{b,S}\right\}}{L} \cdot \sigma_e^2$$
$$+ \frac{(N-\mathcal{N}_p)\cdot\text{trace}\{\mathbf{\Phi}_{b,S}\}}{L\mathcal{N}_p} + \frac{\sigma_w^2}{\alpha\mathcal{N}_p\bar{P}} \quad (20)$$

$$\text{MSE}(\hat{\mathbf{h}}_{DRS})$$
$$= \frac{1}{(2L-1)M}\mathbb{E}\left\{\left\|\hat{\tilde{\mathbf{h}}}_{DRS} - \tilde{\mathbf{h}}_{DRS}\right\|_2^2\right\}$$
$$= \frac{\text{trace}\left\{\left(\left(\mathbf{P}_2^{\text{AF}}\right)^H\mathbf{P}_2^{\text{AF}}\right)^{-1}\mathbf{J}_{DRS}\mathbf{\Phi}_2^{\text{AF}}\right\}}{(2L-1)M} \cdot \sigma_e^2$$
$$+ \frac{N-\mathcal{N}_p}{\mathcal{N}_p}\cdot\frac{\text{trace}\left\{\mathbf{\Phi}_2^{\text{AF}}\right\}}{(2L-1)M} + \frac{\sigma_w^2}{\alpha\mathcal{N}_p\bar{P}}$$
$$\cdot\frac{\sum_{k=1}^{M}\text{trace}\left\{\mathbf{\Phi}_{D,R_k}^{\text{AF}}\right\}}{(2L-1)M} + \frac{M\left(\alpha\bar{P}+\sigma_w^2\right)\sigma_w^2}{\alpha(1-\alpha)\mathcal{N}_p\bar{P}^2} \quad (21)$$

$$\text{MSE}(\hat{\mathbf{h}}_{DR})$$
$$= \frac{1}{Lm}\mathbb{E}\left\{\left\|\hat{\tilde{\mathbf{h}}}_{DR} - \tilde{\mathbf{h}}_{DR}\right\|_2^2\right\}$$
$$= \frac{\text{trace}\left\{\left(\left(\mathbf{P}_2^{\text{DF}}\right)^H\mathbf{P}_2^{\text{DF}}\right)^{-1}\mathbf{J}_{DR}\mathbf{\Phi}_2^{\text{DF}}\right\}}{Lm} \cdot \sigma_e^2$$
$$+ \frac{N-\mathcal{N}_p}{\mathcal{N}_p}\cdot\frac{\text{trace}\left\{\mathbf{\Phi}_2^{\text{DF}}\right\}}{Lm} + \frac{m\sigma_w^2}{(1-\alpha)\mathcal{N}_p\bar{P}} \quad (22)$$

where

$$\mathbf{\Phi}_{b,S} = \mathbb{E}\left\{\tilde{\mathbf{h}}_{b,S}\tilde{\mathbf{h}}_{b,S}^H\right\} \quad (23a)$$

$$\mathbf{J}_{D,S} = \mathbf{J}_{R_k,S}$$
$$= \alpha N\bar{P}\mathbf{F}_{(L)}\mathbf{X}_S^{pH}\mathbf{F}^H\mathbf{\Omega}^2\mathbf{F}\mathbf{X}_S^p\mathbf{F}_{(L)}^H \quad (23b)$$

$$\mathbf{J}_{DRS} = Q_1^2(\alpha)\cdot\text{diag}\{\mathbf{T}_1, \ldots, \mathbf{T}_M\} \quad (23c)$$

$$\mathbf{J}_{DR} = \frac{(1-\alpha)N\bar{P}}{m}\cdot\text{diag}\left\{\mathbf{T}_1^{\text{DF}}, \ldots, \mathbf{T}_m^{\text{DF}}\right\} \quad (23d)$$

$$\mathbf{T}_i^{\text{AF}} = \mathbf{F}_{(2L-1)}\mathbf{X}_{R_i}^{pH}\mathbf{F}^H\mathbf{\Omega}^2\mathbf{F}\mathbf{X}_{R_i}^p\mathbf{F}_{(2L-1)}^H \quad (23e)$$

$$\mathbf{T}_i^{\text{DF}} = \mathbf{F}_{(L)}\mathbf{X}_{R_i}^{pH}\mathbf{F}^H\mathbf{\Omega}^2\mathbf{F}\mathbf{X}_{R_i}^p\mathbf{F}_{(L)}^H. \quad (23f)$$

## IV. EFFECT OF FREQUENCY OFFSET AND CHANNEL ESTIMATION ERRORS ON PEP

The impact on symbol error probability of the frequency offset errors and the channel-estimation errors is analyzed here.

Although the BER of a conventional (noncooperative) OFDM with frequency offset has considerably been studied [28], [29], the application of the BER results to a cooperative OFDM uplink is not straightforward. First, the effective $S \to R \to D$ channel in the AF mode is the convolution of $S \to R$ and $R \to D$ channels. It is proven in [18] that the $S \to R \to D$ channel is not Gaussian. Second, in DF mode, the relays retransmit only if there is no decoding error. Since the OFDM channel is usually a frequency-selective fading channel, some subcarriers may suffer deep fading. If the subcarriers are independently modulated, it is very difficult to correctly decode all the subcarriers.

In this section, the PEP of cooperative OFDM by considering both frequency offset and channel estimation errors is derived. An orthogonal block coding signal matrix $\bar{\mathbf{X}}_S = [\tilde{\mathbf{X}}_S(1), \tilde{\mathbf{X}}_S(2), \ldots, \tilde{\mathbf{X}}_S(T)]$, which is $N \times T$ matrix, is assumed.

### A. PEP for the AF Mode

The probability that $\bar{\mathbf{X}}_S$ will be mistaken for another code $\bar{\mathbf{L}}_S$ is upper bounded by [30]

$$
\mathrm{P}_{\mathrm{r}}^{\mathrm{AF}} \left\{ \bar{\mathbf{X}}_S \to \bar{\mathbf{L}}_S \,|\, 0 < \alpha < 1 \right\}
$$
$$
\leq \left( \prod_{n=0}^{2L-2} \frac{1}{1 + \frac{\bar{\gamma}_{DRS,n}\ell_n}{4}} \right) \left( \prod_{n=0}^{L-1} \frac{1}{1 + \frac{\bar{\gamma}_{DS,n}\ell_n}{4}} \right) \quad (24)
$$

where $\bar{\gamma}_{DS,n}$ and $\bar{\gamma}_{DRS,n}$ represent the SINRs of the $S \to D$ and $S \to R \to D$ channels, respectively, in the $n$th multipath tap, and $\ell_n$ is the $n$th eigenvalue of $(\bar{\mathbf{X}}_S - \bar{\mathbf{L}}_S)(\bar{\mathbf{X}}_S - \bar{\mathbf{L}}_S)^H$. From Appendix I, the SINR of $S \to D$ and $S \to R \to D$ links is given by (25), shown at the bottom of the page. In the high SINR regime with $\sigma_e^2 \to 0$, $\bar{\gamma}_{DS,n}$ and $\bar{\gamma}_{DRS,n}$ can be approximated as

$$
\lim_{\substack{\sigma_e^2 \to 0 \\ \mathrm{SNR} \to \infty}} \bar{\gamma}_{DS,n} \to \alpha \mathrm{SNR} \cdot |\tilde{\mathbf{h}}_{D,S}[n]|^2
$$

$$
\lim_{\substack{\sigma_e^2 \to 0 \\ \mathrm{SNR} \to \infty}} \bar{\gamma}_{DRS,n} \to \frac{\alpha(1-\alpha)\mathrm{SNR} \cdot \left| \sum\limits_{k=1}^{M} \tilde{\mathbf{h}}_{D,R_k,S}[n] \right|^2}{M \left[ \frac{\mathcal{L}_u(M+1)(1-\alpha)}{\alpha} + 1 \right]}
$$

where $\mathrm{SNR} = \bar{P}/\sigma_w^2$ denotes the average signal-to-noise ratio (SNR), and (24) can be rewritten as

$$
\lim_{\substack{\sigma_e^2 \to 0 \\ \mathrm{SNR} \to \infty}} \mathrm{P}_{\mathrm{r}}^{\mathrm{AF}} \left\{ \bar{\mathbf{X}}_S \to \bar{\mathbf{L}}_S \,|\, 0 < \alpha < 1 \right\}
$$
$$
\leq \underbrace{\left( \frac{4 \left[ \frac{\mathcal{L}_u(M+1)(1-\alpha)}{\alpha} + 1 \right]}{\alpha(1-\alpha)\mathrm{SNR}} \right)^{2L-1} \left( \frac{4}{\alpha \mathrm{SNR}} \right)^{L}}_{\text{multipath diversity gain}}
$$
$$
\times \underbrace{\left( \prod_{n=0}^{2L-2} \frac{M}{\left| \sum\limits_{k=1}^{M} \tilde{\mathbf{h}}_{D,R_k,S}[n] \right|^2 \ell_n} \right)}_{\text{multirelay diversity gain}} \left( \prod_{n=0}^{L-1} \frac{1}{\left| \tilde{\mathbf{h}}_{D,S}[n] \right|^2 \ell_n} \right).
$$
$$(26)$$

When $L$ is small, the $M$-order multirelay diversity dominates the diversity gain in a high SINR regime, and a larger $M$ implies a smaller PEP.

### B. PEP for the DF Mode

In DF mode, each relay decodes the received signal from $S$. The relays with decoding errors will not retransmit. By using $P_{\mathrm{relay}}$ to represent the average probability of the decoding error at each relay, the probability that $m$ out of $M$ relays successfully decode the received signal is a binomial distribution, i.e., $P_{\mathrm{relay},m} = \binom{M}{m}(1 - P_{\mathrm{relay}})^m P_{\mathrm{relay}}^{M-m}$. We also use $P_{S \to D}$ to represent the probability of the decoding error at $D$ in the first time slot. $P_{\mathrm{relay}}$ and $P_{S \to D}$ are given, respectively, by

$$
P_{\mathrm{relay}} = \mathrm{P}_{\mathrm{r}} \left\{ \bar{\mathbf{X}}_S \to \bar{\mathbf{L}}_S \,|\, 0 < \alpha < 1; R_k \right\}
$$
$$
\leq \prod_{n=0}^{L-1} \frac{1}{1 + \frac{\bar{\gamma}_{R_k S,n}\ell_n}{4}} \quad (27)
$$
$$
P_{S \to D} = \mathrm{P}_{\mathrm{r}} \left\{ \bar{\mathbf{X}}_S \to \bar{\mathbf{L}}_S \,|\, 0 < \alpha < 1; D \right\}
$$
$$
\leq \prod_{n=0}^{L-1} \frac{1}{1 + \frac{\bar{\gamma}_{DS,n}\ell_n}{4}} \quad (28)
$$

where $\bar{\gamma}_{R_k S,n}$ represents the SINR of the $S \to R_k$ channel in the $n$th tap. From the SINR analysis in Appendix I-A, $\bar{\gamma}_{R_k S,n}$

$$
\bar{\gamma}_{DS,n} = \frac{\alpha \bar{P} \cdot \left| \tilde{\mathbf{h}}_{D,S}[n] \right|^2 \cdot \beta_e}{\sigma_{\mathrm{AF},1}^2 + \left( \alpha \bar{P} \cdot \beta_e + \frac{\sigma_{\mathrm{AF},1}^2}{\left| \tilde{\mathbf{h}}_{D,S}[n] \right|^2} \right) \cdot \mathrm{MSE}(\hat{\tilde{\mathbf{h}}}_{D,S})} \quad (25\mathrm{a})
$$

$$
\bar{\gamma}_{DRS,n} = \frac{\alpha(1-\alpha)\bar{P}^2 \left| \sum\limits_{k=1}^{M} \tilde{\mathbf{h}}_{D,R_k,S}[n] \right|^2 \cdot \beta_e}{M\sigma_{\mathrm{AF},2}^2(\alpha \bar{P} + \sigma_w^2) + M \left( \alpha(1-\alpha)\bar{P}^2 \cdot \beta_e + \frac{M\sigma_{\mathrm{AF},2}^2(\alpha \bar{P} + \sigma_w^2)}{\left| \sum\limits_{k=1}^{M} \tilde{\mathbf{h}}_{D,R_k,S}[n] \right|^2} \right) \cdot \mathrm{MSE}(\hat{\mathbf{h}}_{DRS})} \quad (25\mathrm{b})
$$

is given by

$$\bar{\gamma}_{R_k S,n} = \frac{\alpha \bar{P} \cdot \left| \tilde{\mathbf{h}}_{R_k,S}[n] \right|^2 \cdot \beta_e}{\sigma_{\mathrm{DF},1}^2 + \left( \alpha \bar{P} \cdot \beta_e + \frac{\sigma_{\mathrm{DF},1}^2}{\left| \tilde{\mathbf{h}}_{D,S}[n] \right|^2} \right) \mathrm{MSE}(\hat{\tilde{\mathbf{h}}}_{D,S})}$$

where $\sigma_{\mathrm{DF},1}^2 = (\alpha \pi^2 \sigma_e^2 \bar{P}/3) + \sigma_w^2$.

In the second time slot, the $m$ relays with correct decoding will retransmit. The PEP that $\bar{\mathbf{X}}_S$ will be mistaken for another codeword $\bar{\mathbf{L}}_S$ is upper bounded by

$$\mathrm{P}_{\mathrm{r},m}^{\mathrm{DF}} \left\{ \bar{\mathbf{X}}_S \to \bar{\mathbf{L}}_S \,|\, 0 < \alpha < 1 \right\} \le \prod_{n=0}^{L-1} \frac{1}{1 + \frac{\bar{\gamma}_{DR,m,n}\ell_n}{4}} \quad (29)$$

where $\bar{\gamma}_{DR,m,n}$ represents the SINR of the $R \to D$ channel in the $n$th multipath tap. From Appendix II, we have

$$\bar{\gamma}_{DR,m,n}$$
$$= \frac{(1-\alpha)\bar{P} \cdot \left| \sum_{k=1}^{m} \tilde{\mathbf{h}}_{D,R_k}[n] \right|^2 \cdot \beta_e}{m\sigma_{\mathrm{DF},2}^2 + m \left( \mathcal{L}_u(1-\alpha)\bar{P}\beta_e + \frac{m\sigma_{\mathrm{DF},2}^2}{\left| \sum_{k=1}^{m} \tilde{\mathbf{h}}_{D,R_k}[n] \right|^2} \right) \mathrm{MSE}(\hat{\mathbf{h}}_{DR})}.$$

The averaged PEP of the DF mode is upper bounded by

$$\overline{\mathrm{PEP}^{\mathrm{DF}}} \le P_{S \to D} \cdot \sum_{m=0}^{M} P_{\mathrm{relay},m} \mathrm{P}_{\mathrm{r},m}^{\mathrm{DF}} \left\{ \bar{\mathbf{X}}_S \to \bar{\mathbf{L}}_S \,|\, 0 < \alpha < 1 \right\}. \quad (30)$$

In the high SINR regime with $\sigma_e^2 \to 0$, (29) can be approximated as

$$\lim_{\substack{\sigma_e^2 \to 0 \\ \mathrm{SNR} \to \infty}} \mathrm{P}_{\mathrm{r}}^{\mathrm{DF}} \left\{ \bar{\mathbf{X}}_S \to \bar{\mathbf{L}}_S \,|\, 0 < \alpha < 1 \right\}$$

$$\le \underbrace{\left( \frac{4}{(1-\alpha)\mathrm{SNR}} \right)^L}_{\text{multipath diversity gain}} \times \underbrace{\left( \prod_{n=0}^{L-1} \frac{m}{\left| \sum_{k=1}^{m} \tilde{\mathbf{h}}_{D,R_k}[n] \right|^2 \ell_n} \right)}_{\text{multirelay diversity gain}}. \quad (31)$$

A comparison of (26) and (31) shows that for a given $M$, in a high SINR regime with $\sigma_e^2 \to 0$, the AF mode outperforms the DF mode in terms of diversity gain. However, in real systems, the DF mode usually outperforms the AF mode because of the following reasons. First, Lemmas 1 and 2 tell us that for a given $L$, the maximum number of active relays used in the DF mode is almost twice that of the AF mode, and the achievable cooperative diversity gain in the DF mode is much higher than that obtained in the AF mode. Second, by considering the frequency offset, the OFDM transmission is usually interference limited, and the diversity gain obtained in the AF mode may be deteriorated by the interference and noise that accumulated in the relays. The interference-mitigation capability in DF mode provides a performance advantage over the AF mode in the low SINR regime. A brief performance comparison between the AF and DF modes is shown in Table I.

TABLE I
PERFORMANCE COMPARISON BETWEEN AF AND DF MODES

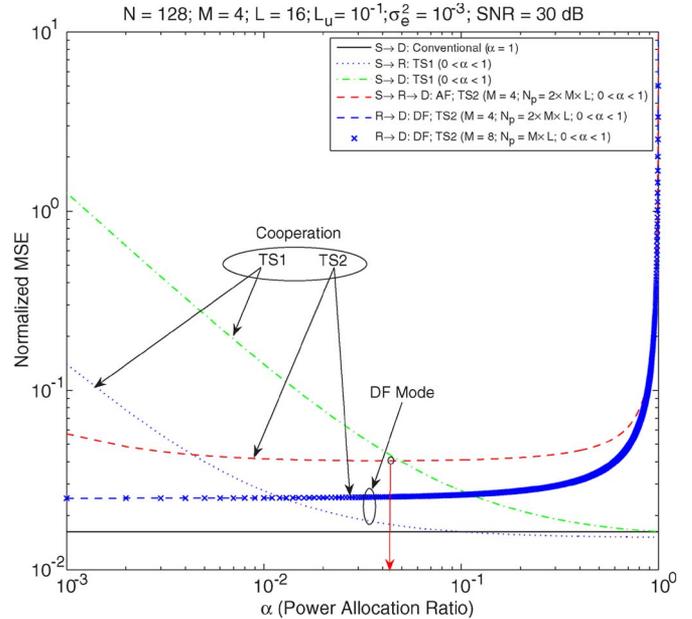| Relaying Mode | AF | DF |
|---|---|---|
| Complexity | Low | High |
| Channel Estimation Accuracy | Low | High |
| Maximum Concatenated Channel Delay | $2L_{max} - 1$ | $L_{max}$ |
| Maximum Number of Relays | $\frac{N}{2L_{max}-1}$ | $\frac{N}{L_{max}}$ |
| Capability to Combat Multipath-fading | Low | High |
| Achievable Diversity Gain | Low | High |
| PEP | High | Low |



Fig. 2. Normalized MSE of channel estimation in either conventional transmission ($\alpha = 1$) or the proposed cooperative transmission ($0 < \alpha < 1$).

## V. NUMERICAL RESULTS

The PEP performance of the proposed channel estimation schemes in the presence of frequency offsets is evaluated in this section. By keeping the total power consumption constant, the PEP performance as a function of power allocation ratio $\alpha$ is first evaluated. The performance comparison between the proposed pilot designs for the AF and DF relaying modes is then performed for different channel lengths $L$. After that, the PEP performance as a function of frequency offset variance, i.e., $\sigma_\epsilon^2$, is evaluated. Finally, for a given $\sigma_\epsilon^2$, the PEP performance as the SNR increases is simulated.

Only uniform power-delay profiles are considered for brevity, i.e., $\mathbb{E}\{|h_{R_k,S}(l)|^2\} = 1/L$ and $\mathbb{E}\{|h_{D,R_k}(l)|^2\} = \mathbb{E}\{|h_{D,S}(l)|^2\} = \mathcal{L}_u/L$, where $l = 0, 1, 2, \ldots, L-1$. The number of subcarriers is $N = 128$. The SNR of the pilot subcarriers is $\mathrm{SNR} = \bar{P}/\sigma_w^2$. Identical average powers are assigned to both pilot and data subcarriers. Independent and identically distributed (i.i.d.) frequency offset estimation errors are assumed for $S \to R$, $R \to D$, and $S \to R \to D$ channels with a variance of $\sigma_e^2$.

The normalized MSE for channel estimation is shown as a function of the power allocation ratio (see Fig. 2). The MSEs of the $S \to R$ and $S \to D$ links are monotonically decreasing functions of $\alpha$, whereas those for the $S \to R \to D$ (for the AF mode) and $R \to D$ (for the DF mode) links are monotonically
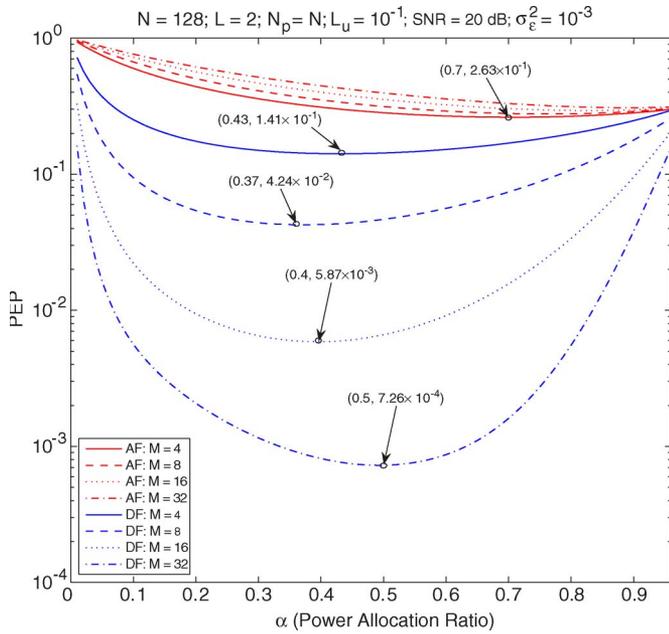
Fig. 3. PEP of the proposed cooperative transmission with $L_{\max} = 2$ and $\sigma_e^2 = 10^{-3}$.

increasing functions of $\alpha$. Although the normalized MSE for the $R \to D$ link in DF mode is always smaller than that for the $S \to R \to D$ link in AF mode for each $\alpha$, this result does not mean that the DF mode always outperforms the AF mode in terms of channel estimation error, because the estimation error in the $S \to R$ link for the DF mode also contributes some impairments to the decoding. However, in each relaying mode, an optimal $\alpha$ can be found to optimize the performance of the relay OFDM system.

The PEP performance of the proposed cooperative transmission in the presence of both frequency offset and channel-estimation errors is illustrated in Figs. 3–7. From Section III-C, the channel-estimation MSE is a function of the variance of the frequency offset estimation error (i.e., $\sigma_e^2$) so that we use $\sigma_e^2$ as the only parameter of impairment. For Figs. 3–5, $\mathcal{L}_u$ is set to $10^{-1}$. All the eigenvalues of $(\bar{\mathbf{X}}_S - \bar{\mathbf{L}}_S)(\bar{\mathbf{X}}_S - \bar{\mathbf{L}}_S)^H$ are set to 1.

The performances of the AF and DF modes are compared for $L = 2$ and $\sigma_e^2 = 10^{-3}$ in Fig. 3. Since the DF spatial diversity gain is proportional to the number of relays $M$, a larger number of active relays results in a lower PEP. In contrast, a larger number of AF relays results in a worse PEP performance. This difference can be explained as follows. In AF mode, interference and noise accumulate in each relay, and the interference due to frequency offset is not Gaussian when $\sigma_e^2$ is large. Since this interference cannot be averaged out by using more relays, the diversity gain will deteriorate by this process of accumulation. However, the DF mode eliminates the interference and noise. It is this interference-mitigation capability that guarantees that the DF mode will achieve a better PEP performance with more relays. When $M = 16$ and 32, the PEP performances of the AF mode are monotonically decreasing functions of the power-allocation ratio. That is, the AF mode cannot improve the diversity gain through cooperative transmission. However, when $M < 16$, it achieves a diversity gain. For each $M$, an
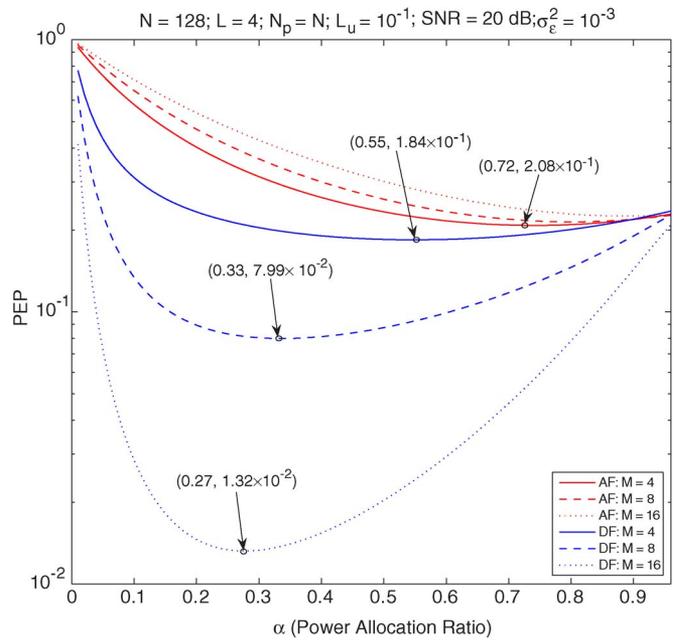


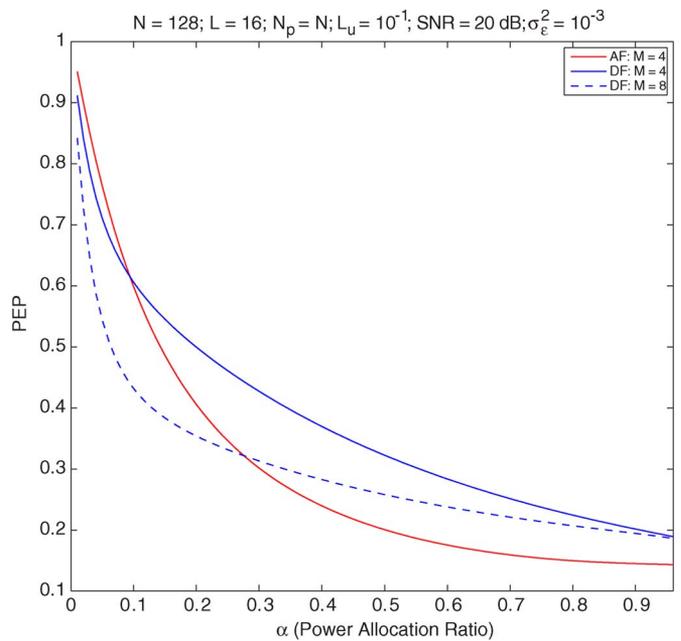Fig. 4. PEP of the proposed cooperative transmission with $L_{\max} = 4$ and $\sigma_e^2 = 10^{-3}$.



Fig. 5. PEP of the proposed cooperative transmission with $L_{\max} = 16$ and $\sigma_e^2 = 10^{-3}$.

optimal $\alpha$ that minimizes the PEP can be found. As compared with the AF mode, the DF mode can always achieve a diversity gain for each $M$.

Although the optimal PEP performance improves as the number of relays increases, increasing too many results in a degradation. This finding can be explained as follows. For a small number of relays, the performance is noise and/or interference limited, and the effective SINR of the $S \to R \to D$ channels can be improved by increasing the number of relays. As the number of relays increases, the power allocation to each relay decreases, and the cooperation becomes power limited
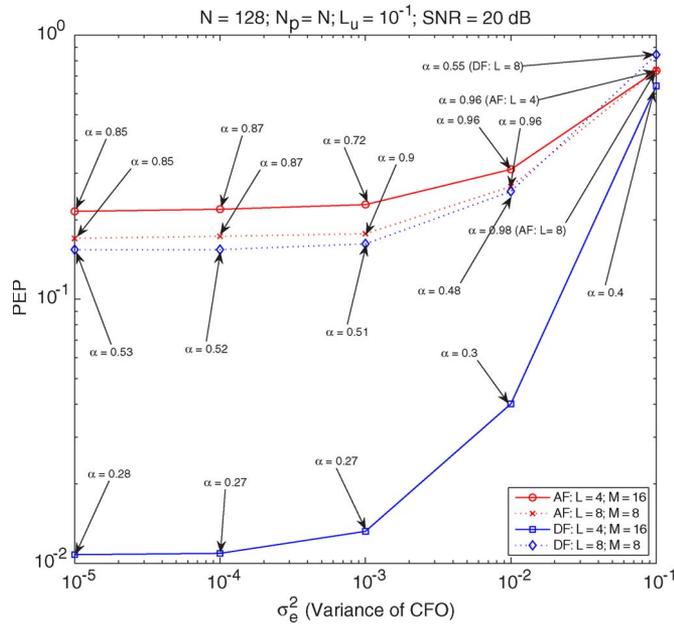
Fig. 6.   PEP of the proposed cooperative transmission as a function of $\sigma_e^2$ with $L_{\max} = 4$ and 8.
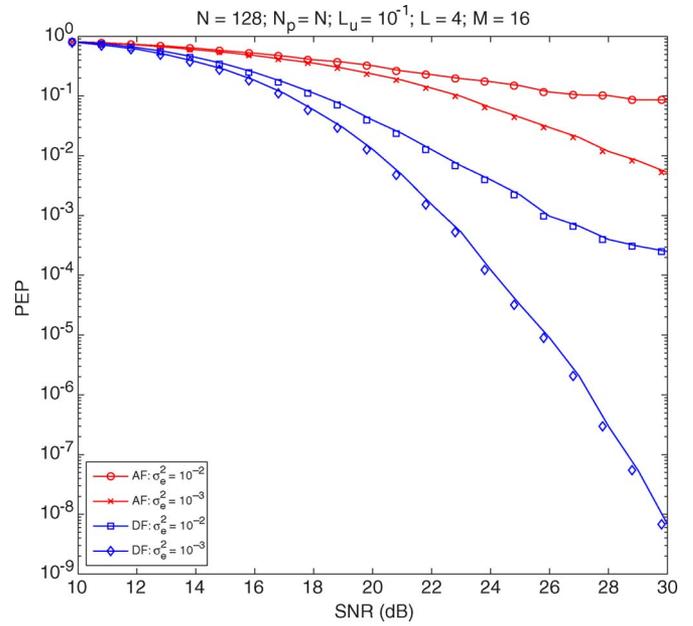


Fig. 7.   PEP of the proposed cooperative transmission as a function of SNR with $\sigma_e^2 = 10^{-3}$ and $L_{\max} = 4$ and 8.

once the number of relays is beyond a threshold. The effective SINR of the $S \rightarrow R \rightarrow D$ channels becomes lower in a power-limited environment if more relays are used.

For a fixed $\sigma_e^2 = 10^{-3}$, but the channel order is increasing to 4 and 16, the PEP performance is shown in Figs. 4 and 5, respectively. When $L = 4$, the optimal $(M, \alpha)$ can always be found to make the DF mode outperform the AF mode in terms of PEP performance. Note that for each relaying mode, a larger channel order results in a higher interference and noise in the $S \rightarrow R$, $R \rightarrow D$, $S \rightarrow D$, and $S \rightarrow R \rightarrow D$ channels. This higher interference and noise degrade the SINR. However, for a given number of relays, since a $(2L - 1)$-order multipath diversity gain can be obtained in the AF mode [see (24)], this gain may compensate for the performance loss due to SINR degradation. When the channel order is not large (e.g., in this simulation, $L < 16$ is required), the multipath diversity gain dominates the performance of the AF mode, and the PEP performance may be improved as the channel order increases. If the channel order increases (e.g., to 16), the cooperation channel becomes power limited, and the SINR degradation in each tap will deteriorate the multipath diversity gain. Increasing the channel order degrades the PEP performance in the DF mode, because this mode can only obtain a $L$-order multipath diversity gain, as shown in (30).

The PEP performance as a function of $\sigma_e^2$ is shown in Fig. 6, which considers $(L = 4, M = 16)$ and $(L = 8, M = 8)$. Both AF and DF mode PEPs monotonically increase with $\sigma_e^2$. For each number of relays, the DF mode always outperforms the AF mode for a small $\sigma_e^2$, although both modes approach the same PEP performance for a large $\sigma_e^2$ (i.e., the system is interference rather than noise limited, and the diversity gain cannot be improved through cooperation).

The PEP performances as functions of SNR are shown in Fig. 7 for $L = 4$, $M = 16$, and $\sigma_e^2 = 10^{-2}$ and $10^{-3}$. Since the system is noise limited for a small $\sigma_e^2$ ($\sigma_e^2 = 10^{-3}$), the relays

realize the spatial diversity gain. The PEP performance of the DF mode is about 9 dB better than that of the AF mode at an error rate of $5 \times 10^{-3}$. As $\sigma_e^2$ increases to $10^{-2}$, the system becomes interference limited, and an error floor appears in both AF and DF modes. In this environment, the performance increases to about 11.3 dB, i.e., the DF mode has a higher interference-mitigation capability than the AF mode.

## VI. Conclusion

Channel estimation for cooperative AF or DF OFDM systems in the presence of frequency offsets has been considered. A two-time-slot cooperative channel-estimation protocol has been proposed. For a given channel order $L$, the maximum number of AF and DF relays was constrained to be $\lfloor N/(2L - 1) \rfloor$ and $\lfloor N/L \rfloor$, respectively. As a result, the latter achieves more diversity gain than the former. The PEP performance of an orthogonal block code in the proposed cooperative transmission was also evaluated by considering both frequency offset and channel-estimation errors. The optimal power allocation between the source and a set of relays (AF or DF) was derived to minimize the PEP. For both relaying modes, a larger channel order results in increased interference and noise, which degrade the SINR. Since the AF mode can realize a $(2L - 1)$-order multipath diversity gain, it performs better as the channel order increases provided that the channel order is not too large. Unlike AF relays, DF relays will suffer a PEP performance degradation when the channel order increases, because the $L$-order multipath diversity gain cannot compensate for the SINR loss. Interference will increase if more relays are used in the AF mode, which results in degradation of performance. The interference-mitigation capability of the DF mode improves performance by allowing the use of more relays, and when the channel order is smaller than 16, they outperform AF relays in terms of PEP.

## APPENDIX I
## SINR ANALYSIS IN AF

*First Time Slot*

Without loss of generality, we assume that $\hat{\tilde{\mathbf{h}}}_{D,S} = \tilde{\mathbf{h}}_{D,S} + \Delta\tilde{\mathbf{h}}_{D,S}$, where $\Delta\tilde{\mathbf{h}}_{D,S}$ represents the estimation error of $\tilde{\mathbf{h}}_{D,S}$. The received vector $\mathbf{y}_{D,1}$ can be demodulated as

$$
\begin{aligned}
\mathbf{r}_{D,1} &= \mathbf{F}^H \mathbf{y}_{D,1} = \sqrt{\alpha N \bar{P}} \mathbf{E}_{D,S}^{\text{cir}} \mathbf{X}_S \mathbf{F}_{(L)}^H \tilde{\mathbf{h}}_{D,S} + \mathbf{F}^H \mathbf{w}_{D,1} \\
&= \underbrace{\sqrt{\alpha N \bar{P}} \mathbf{E}_{D,S}^{\text{diag}} \mathbf{X}_S \mathbf{F}_{(L)}^H \tilde{\mathbf{h}}_{D,S}}_{\boldsymbol{\mu}_{D,1}} \\
&\quad + \underbrace{\underbrace{\sqrt{\alpha N \bar{P}} \mathbf{E}_{D,S}^{\text{off}} \mathbf{X}_S \mathbf{F}_{(L)}^H \tilde{\mathbf{h}}_{D,S}}_{\text{interference}} + \mathbf{F}^H \mathbf{w}_{D,1}}_{\boldsymbol{\xi}_{D,1}}
\end{aligned} \tag{32}
$$

where we decompose $\mathbf{E}_{D,S}^{\text{cir}}$ as $\mathbf{E}_{D,S}^{\text{cir}} = \mathbf{E}_{D,S}^{\text{diag}} + \mathbf{E}_{D,S}^{\text{off}}$, with $\mathbf{E}_{D,S}^{\text{diag}}$ being a diagonal matrix that $[\mathbf{E}_{D,S}^{\text{diag}}]_{ii} = [\mathbf{E}_{D,S}^{\text{cir}}]_{ii}$, and $\mathbf{E}_{D,S}^{\text{off}}$ comprising all the off-diagonal elements of $\mathbf{E}_{D,S}^{\text{cir}}$, $\boldsymbol{\mu}_{D,1}$ is the useful signal of $\mathbf{r}_{D,1}$, and $\boldsymbol{\xi}_{D,1}$ represents the interference plus noise of $\mathbf{r}_{D,1}$.

The signal of the $n$th tap can be demodulated as

$$
\frac{\hat{\tilde{\mathbf{h}}}_{D,S}^*[n] \cdot \mathbf{r}_{D,1}[n]}{\left|\hat{\tilde{\mathbf{h}}}_{D,S}[n]\right|^2} = \frac{\tilde{\mathbf{h}}_{D,S}^*[n] \cdot \boldsymbol{\mu}_{D,1}[n]}{\left|\hat{\tilde{\mathbf{h}}}_{D,S}[n]\right|^2} + \frac{\Delta\tilde{\mathbf{h}}_{D,S}^*[n] \cdot \boldsymbol{\mu}_{D,1}[n]}{\left|\hat{\tilde{\mathbf{h}}}_{D,S}[n]\right|^2} + \frac{\hat{\tilde{\mathbf{h}}}_{D,S}^*[n] \cdot \boldsymbol{\xi}_{D,1}[n]}{\left|\hat{\tilde{\mathbf{h}}}_{D,S}[n]\right|^2}. \tag{33}
$$

The SINR of (33) is given by

$$
\bar{\gamma}_{DS,n} = \frac{\mathbb{E}\left\{\left|\tilde{\mathbf{h}}_{D,S}^*[n] \cdot \boldsymbol{\mu}_{D,1}[n]\right|^2\right\}}{\mathbb{E}\left\{\left|\Delta\tilde{\mathbf{h}}_{D,S}^*[n] \cdot \boldsymbol{\mu}_{D,1}[n]\right|^2 + \left|\hat{\tilde{\mathbf{h}}}_{D,S}^*[n] \cdot \boldsymbol{\xi}_{D,1}[n]\right|^2\right\}}. \tag{34}
$$

From [13, App. I], (34) can be simplified as

$$
\bar{\gamma}_{DS,n} = \frac{\alpha\bar{P} \cdot \left|\tilde{\mathbf{h}}_{D,S}[n]\right|^2 \cdot \beta_e}{\sigma_{\text{AF},1}^2 + \left(\alpha\bar{P} \cdot \beta_e + \frac{\sigma_{\text{AF},1}^2}{\left|\tilde{\mathbf{h}}_{D,S}[n]\right|^2}\right) \cdot \text{MSE}(\hat{\tilde{\mathbf{h}}}_{D,S})} \tag{35}
$$

where $\beta_e = 1 - (\pi^2 \sigma_e^2/3) + (\pi^4 \sigma_e^4/20)$, and $\sigma_{\text{AF},1}^2 = (\mathcal{L}_u \alpha \pi^2 \sigma_e^2 \bar{P}/3) + \sigma_w^2$.

*Second Time Slot*

The received vector $\mathbf{y}_{D,2}^{\text{AF}}$ can be demodulated as in

$$
\begin{aligned}
\mathbf{r}_{D,2}^{\text{AF}} &= \mathbf{F}^H \mathbf{y}_{D,2}^{\text{AF}} \\
&= \underbrace{\sum_{k=1}^M Q_1(\alpha) \mathbf{E}_{D,R_k,S}^{\text{diag}} \mathbf{X}_S \mathbf{F}_{(2L-1)}^H \tilde{\mathbf{h}}_{D,R_k,S}}_{\boldsymbol{\mu}_{D,2}^{\text{AF}}} \\
&\quad + \underbrace{\boldsymbol{I}_{D,R_k,S} + \sum_{k=1}^M Q_2(\alpha) \mathbf{E}_{D,R_k}^{\text{cir}} \mathbf{W}_\eta \mathbf{F}_{(L)}^H \tilde{\mathbf{h}}_{D,R_k} + \mathbf{F}^H \mathbf{w}_{D,2}}_{\boldsymbol{\xi}_{D,2}^{\text{AF}}}
\end{aligned} \tag{36}
$$

where $\boldsymbol{I}_{D,R_k,S} = \sum_{k=1}^M Q_1(\alpha) \mathbf{E}_{D,R_k,S}^{\text{off}} \mathbf{X}_S \mathbf{F}_{(2L-1)}^H \tilde{\mathbf{h}}_{D,R_k,S}$, and $\mathbf{E}_{D,R_k,S}^{\text{cir}} = \mathbf{E}_{D,R_k,S}^{\text{diag}} + \mathbf{E}_{D,R_k,S}^{\text{off}}$. Similar to Appendix I-A, the SINR of (36) is given by (37), shown at the bottom of the page. From [13, App. II], (37) can be simplified as (38), shown at the bottom of the page, where

$$
\begin{aligned}
\sigma_{\text{AF},2}^2 &= \frac{2\mathcal{L}_u(M^2 - M + 1)\alpha(1-\alpha)\pi^2 \sigma_e^2 \bar{P}^2}{3M(\alpha\bar{P} + \sigma_w^2)} \\
&\quad + \frac{\mathcal{L}_u \alpha \pi^2 \sigma_e^2 \bar{P}}{3} + \frac{\mathcal{L}_u(M+1)(1-\alpha)\bar{P}\sigma_w^2}{\alpha\bar{P} + \sigma_w^2} + \sigma_w^2.
\end{aligned}
$$

$$
\bar{\gamma}_{DS,n} = \frac{\mathbb{E}\left\{\left|\left(\sum_{k=1}^M \tilde{\mathbf{h}}_{D,R_k,S}[n]\right)^* \cdot \boldsymbol{\mu}_{D,2}^{\text{AF}}[n]\right|^2\right\}}{\mathbb{E}\left\{\left|\left(\sum_{k=1}^M \Delta\tilde{\mathbf{h}}_{D,R_k,S}[n]\right)^* \cdot \boldsymbol{\mu}_{D,2}^{\text{AF}}[n]\right|^2\right\} + \mathbb{E}\left\{\left|\left(\sum_{k=1}^M \hat{\tilde{\mathbf{h}}}_{D,R_k,S}[n]\right)^* \cdot \boldsymbol{\xi}_{D,2}^{\text{AF}}[n]\right|^2\right\}} \tag{37}
$$

$$
\bar{\gamma}_{DRS,n} = \frac{\alpha(1-\alpha)\bar{P}^2 \left|\sum_{k=1}^M \tilde{\mathbf{h}}_{D,R_k S}[n]\right|^2 \cdot \beta_e}{M\sigma_{\text{AF},2}^2(\alpha\bar{P} + \sigma_w^2) + M\left(\alpha(1-\alpha)\bar{P}^2 \cdot \beta_e + \frac{M\sigma_{\text{AF},2}^2(\alpha\bar{P}+\sigma_w^2)}{\left|\sum_{k=1}^M \tilde{\mathbf{h}}_{D,R_k S}[n]\right|^2}\right) \cdot \text{MSE}(\hat{\mathbf{h}}_{DR})} \tag{38}
$$

$$
\bar{\gamma}_{DR,m,n} = \frac{\mathbb{E}\left\{\left|\left(\sum_{k=1}^{m}\tilde{\mathbf{h}}_{D,R_k}[n]\right)^{*}\cdot\boldsymbol{\mu}_{D,2}^{\mathrm{DF}}[n]\right|^2\right\}}{\mathbb{E}\left\{\left|\left(\sum_{k=1}^{m}\Delta\tilde{\mathbf{h}}_{D,R_k}[n]\right)^{*}\cdot\boldsymbol{\mu}_{D,2}^{\mathrm{DF}}[n]\right|^2\right\} + \mathbb{E}\left\{\left|\left(\sum_{k=1}^{m}\hat{\tilde{\mathbf{h}}}_{D,R_k}[n]\right)^{*}\cdot\boldsymbol{\xi}_{D,2}^{\mathrm{DF}}[n]\right|^2\right\}}
$$

$$
= \frac{(1-\alpha)\bar{P}\cdot\left|\sum_{k=1}^{m}\tilde{\mathbf{h}}_{D,R_k}[n]\right|^2\cdot\beta_e}{m\sigma_{\mathrm{DF},2}^2 + m\left(\mathcal{L}_u(1-\alpha)\bar{P}\cdot\beta_e + \frac{m\sigma_{\mathrm{DF},2}^2}{\left|\sum_{k=1}^{m}\tilde{\mathbf{h}}_{D,R_k}[n]\right|^2}\right)\cdot\mathrm{MSE}(\hat{\mathbf{h}}_{DR})} \tag{40}
$$

## APPENDIX II
## SINR ANALYSIS IN DF

The received vector $\mathbf{y}_{D,2}^{\mathrm{DF}}$ can be demodulated as

$$
\mathbf{r}_{D,2}^{\mathrm{DF}} = \underbrace{\sum_{k=1}^{m}\sqrt{\frac{(1-\alpha)N\bar{P}}{m}}\mathbf{E}_{D,R_k}^{\mathrm{diag}}\mathbf{X}_{R_k}\mathbf{F}_{(L)}^{H}\tilde{\mathbf{h}}_{D,R_k}}_{\boldsymbol{\mu}_{D,2}^{\mathrm{DF}}}
$$
$$
+\underbrace{\sum_{k=1}^{m}\sqrt{\frac{(1-\alpha)N\bar{P}}{m}}\mathbf{E}_{D,R_k}^{\mathrm{off}}\mathbf{X}_{R_k}\mathbf{F}_{(L)}^{H}\tilde{\mathbf{h}}_{D,R_k}+\mathbf{F}^{H}\mathbf{w}_{D,2}}_{\text{interference}} \cdot
$$
$$
\underbrace{\phantom{x}}_{\boldsymbol{\xi}_{D,2}^{\mathrm{DF}}} \tag{39}
$$

Similar to the SINR analysis in Appendix I, the SINR of (39) in the $n$th tap is given by (40), shown at the top of the page, where $\sigma_{\mathrm{DF},2}^2 = (\mathcal{L}_u(1-\alpha)\pi^2\sigma_e^2\bar{P}/3) + \sigma_w^2$.

## REFERENCES

[1] T. Cover and A. E. Gamal, "Capacity theorems for the relay channel," *IEEE Trans. Inf. Theory*, vol. IT-25, no. 5, pp. 572–584, Sep. 1979.

[2] J. N. Laneman and G. W. Wornell, "Distributed space–time-coded protocols for exploiting cooperative diversity in wireless networks," *IEEE Trans. Inf. Theory*, vol. 49, no. 10, pp. 2415–2425, Oct. 2003.

[3] A. Sendonaris, E. Erkip, and B. Aazhang, "Increasing uplink capacity via user cooperation diversity," in *Proc. IEEE ISIT*, Cambridge, MA, Aug. 1998, p. 156.

[4] X. Guo, W. Ma, Z. Guo, X. Shen, and Z. Hou, "Adaptive resource reuse scheduling for multihop relay wireless network based on multicoloring," *IEEE Commun. Lett.*, vol. 12, no. 3, pp. 176–178, Mar. 2008.

[5] A. Sendonaris, E. Erkip, and B. Aazhang, "User cooperation diversity. Part I: System description," *IEEE Trans. Commun.*, vol. 51, no. 11, pp. 1927–1938, Nov. 2003.

[6] R. U. Nabar, H. Bolcskei, and F. W. Kneubuhler, "Fading relay channels: Performance limits and space–time signal design," *IEEE J. Sel. Areas Commun.*, vol. 22, no. 6, pp. 1099–1109, Aug. 2004.

[7] M. Yu and J. Li, "Is amplify-and-forward practically better than decode and-forward or vice versa?" in *Proc. IEEE ICASSP*, Mar. 2005, vol. 3, pp. 365–368.

[8] Z. Yi and I.-M. Kim, "Joint optimization of relay-precoders and decoders with partial channel side information in cooperative networks," *IEEE J. Sel. Areas Commun.*, vol. 25, no. 2, pp. 447–458, Feb. 2007.

[9] IEEE P802.11n/D3.00, *Wireless Lan Medium Access Control (MAC) and Physical Layer (PHY) Specifications: Amendment 3: Enhancements for Higher Throughput*, Sep. 2007.

[10] T. K. Paul and T. Ogunfunmi, "Wireless LAN comes of age: Understanding the IEEE 802.11n amendment," *IEEE Circuits Syst. Mag.*, vol. 8, no. 1, pp. 28–54, First Quarter 2008.

[11] B. Can, H. Yomo, and E. De Carvalho, "Hybrid forwarding scheme for cooperative relaying in OFDM based networks," in *Proc. IEEE Int. Control Conf.*, Istanbul, Turkey, Jun. 2006, vol. 10, pp. 4520–4525.

[12] T. C.-Y. Ng and W. Yu, "Joint optimization of relay strategies and resource allocations in cooperative cellular networks," *IEEE J. Sel. Areas Commun.*, vol. 25, no. 2, pp. 328–339, Feb. 2007.

[13] Z. Zhang, C. Tellambura, and R. Schober, "Improved OFDMA uplink transmission via cooperative relaying in the presence of frequency offsets—Part I: Ergodic information rate analysis," *Eur. Trans. Telecommun.*, under review.

[14] Z. Zhang, C. Tellambura, and R. Schober, "Improved OFDMA uplink transmission via cooperative relaying in the presence of frequency offsets—Part II: Outage information rate analysis," *Eur. Trans. Telecommun.*, under review.

[15] D. Sreedhar and A. Chockalingam, "ICI-ISI mitigation in cooperative SFBC-OFDM with carrier frequency offset," in *Proc. IEEE Int. Symp. PIMRC*, Athens, Greece, Sep. 2007, pp. 1–5

[16] R. Raghunath and A. Chockalingam, "SIR analysis and interference cancellation in uplink OFDMA with large carrier frequency and timing offsets," in *IEEE Wireless Commun. Netw. Conf.*, Kowloon, China, Mar. 2007, pp. 996–1001.

[17] C. Patel, G. Stuber, and T. Pratt, "Statistical properties of amplify and forward relay fading channels," *IEEE Trans. Veh. Technol.*, vol. 55, no. 1, pp. 1–9, Jan. 2006.

[18] C. Patel and G. Stuber, "Channel estimation for amplify and forward relay based cooperation diversity systems," *IEEE Trans. Wireless Commun.*, vol. 6, no. 6, pp. 2348–2356, Jun. 2007.

[19] I. Barhumi, G. Leus, and M. Moonen, "Optimal training design for MIMO OFDM systems in mobile wireless channels," *IEEE Trans. Signal Process.*, vol. 51, no. 6, pp. 1615–1624, Jun. 2003.

[20] H. Minn, N. Al-Dhahir, and Y. Li, "Optimal training signals for MIMO OFDM channel estimation in the presence of frequency offset and phase noise," *IEEE Trans. Commun.*, vol. 54, no. 10, pp. 1754–1759, Oct. 2006.

[21] M. Ghogho and A. Swami, "Training design for multipath channel and frequency-offset estimation in MIMO systems," *IEEE Trans. Signal Process.*, vol. 54, no. 10, pp. 3957–3965, Oct. 2006.

[22] Z. Zhang, W. Zhang, and C. Tellambura, "MIMO-OFDM channel estimation in the presence of frequency offsets," *IEEE Trans. Wireless Commun.*, vol. 7, no. 6, pp. 2329–2339, Jun. 2008.

[23] R. A. Iltis, S. Mirzaei, R. Kastner, R. E. Cagley, and B. T. Weals, "GEN05-4: Carrier offset and channel estimation for cooperative MIMO sensor networks," in *Proc. IEEE GLOBECOM*, San Francisco, CA, Nov. 2006, pp. 1–5.

[24] K. Kim, H. Kim, and H. Park, "OFDM channel estimation for the amply-and-forward cooperative channel," in *Proc. IEEE Veh. Technol. Conf.*, Dublin, Ireland, Apr. 2007, pp. 1642–1646.

[25] O. S. Shin, A. M. Chan, H. T. Kung, and V. Tarokh, "Design of an OFDM cooperative space–time diversity system," *IEEE Trans. Veh. Technol.*, vol. 56, no. 4, pp. 2203–2215, Jul. 2007.

[26] N. Benvenuto, S. Tomasin, and D. Veronesi, "Multiple frequency offsets estimation and compensation for cooperative networks," in *Proc. IEEE Wireless Commun. Netw. Conf.*, Kowloon, China, Mar. 2007, pp. 891–895.

[27] Z. Zhang, W. Zhang, and C. Tellambura, "OFDMA uplink frequency offset estimation via cooperative relaying," *IEEE Trans. Wireless Commun.*, under revision.

[28] L. Rugini and P. Banelli, "BER of OFDM systems impaired by carrier frequency offset in multipath fading channels," *IEEE Trans. Wireless Commun.*, vol. 4, no. 5, pp. 2279–2288, Sep. 2005.

[29] M. Krondorf, T. J. Liang, and G. Fettweis, "Symbol error rate of OFDM systems with carrier frequency offset and channel estimation error in frequency selective fading channels," in *Proc. IEEE Int. Control Conf.*, Glasgow, U.K., Jun. 2007, pp. 5132–5136.

[30] H. Mheidat, M. Uysal, and N. Al-Dhahir, "Equalization techniques for distributed space–time block codes with amplify-and-forward relaying," *IEEE Trans. Signal Process.*, vol. 55, no. 5, pp. 1839–1852, May 2007.

**Wei Zhang** (S'04) received the B.E. and M.E. degrees in control engineering from Shandong University, Jinan, China, in 2000 and 2004, respectively. She is currently working toward the Ph.D. degree with the Department of Electrical and Computer Engineering, University of Alberta, Edmonton, AB, Canada.

Her current research interests include wireless communications theory, signal detection and estimation, and diversity and cooperative communications.

**Chintha Tellambura** (SM'02) received the B.Sc. degree (with first-class honors) from the University of Moratuwa, Moratuwa, Sri Lanka, in 1986, the M.Sc. degree in electronics from the University of London, London, U.K., in 1988, and the Ph.D. degree in electrical engineering from the University of Victoria, Victoria, BC, Canada, in 1993.

He was a Postdoctoral Research Fellow with the University of Victoria, from 1993 to 1994 and with the University of Bradford, West Yorkshire, U.K., from 1995 to 1996. From 1997 to 2002, he was with Monash University, Melbourne, Australia. He is currently a Professor with the Department of Electrical and Computer Engineering, University of Alberta, Edmonton, AB, Canada. His research interests include diversity and fading countermeasures, multiple-input–multiple-output systems and space–time coding, and orthogonal frequency-division multiplexing.

Prof. Tellambura is an Associate Editor for the IEEE TRANSACTIONS ON COMMUNICATIONS and an Area Editor for Wireless Communications Systems and Theory of the IEEE TRANSACTIONS ON WIRELESS COMMUNICATIONS. He was the Chair of the Communication Theory Symposium at Globecom'05 held in St. Louis, MO.

**Zhongshan Zhang** (M'04) received the M.S. degree in computer science and the Ph.D. degree in electrical engineering from the Beijing University of Posts and Telecommunications, Beijing, China, in 2001 and 2004, respectively.

In August 2004, he was an Associate Researcher with DoCoMo Beijing Laboratories, where he was promoted to Researcher in December 2005. Since February 2006, he has been a Postdoctoral Fellow with the University of Alberta, Edmonton, AB, Canada. His main research interests include statistical signal processing, synchronization and channel estimation in multiple-input–multiple-output orthogonal frequency-division multiplexing systems, and cooperative communications.